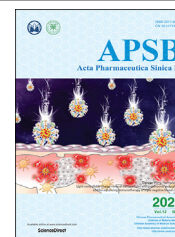




Chinese Pharmaceutical Association  
Institute of Materia Medica, Chinese Academy of Medical Sciences

Acta Pharmaceutica Sinica B

[www.elsevier.com/locate/apsb](http://www.elsevier.com/locate/apsb)  
[www.sciencedirect.com](http://www.sciencedirect.com)



## REVIEW

# Pure drug nano-assemblies: A facile carrier-free nanoplatform for efficient cancer therapy



Shuwen Fu<sup>a,†</sup>, Guanting Li<sup>b,†</sup>, Wenli Zang<sup>c</sup>, Xinyu Zhou<sup>d</sup>, Kexin Shi<sup>e</sup>,  
Yinglei Zhai<sup>e,\*</sup>

<sup>a</sup>School of Pharmacy, Shenyang Pharmaceutical University, Shenyang 110016, China

<sup>b</sup>Department of Pharmaceutics, Wuyi College of Innovation, Shenyang Pharmaceutical University, Shenyang 110016, China

<sup>c</sup>Department of Periodontology, School and Hospital of Stomatology, China Medical University, Liaoning Provincial Key Laboratory of Oral Disease, Shenyang 110016, China

<sup>d</sup>Bio-system Pharmacology, Graduate School of Medicine, Faculty of Medicine, Osaka University, Osaka 565-0871, Japan

<sup>e</sup>Department of Biomedical Engineering, School of Medical Device, Shenyang Pharmaceutical University, Shenyang 110016, China

Received 29 April 2021; received in revised form 24 June 2021; accepted 7 July 2021

### KEY WORDS

Nanotechnology;

**Abstract** Nanoparticulate drug delivery systems (Nano-DDSs) have emerged as possible solution to the obstacles of anticancer drug delivery. However, the clinical outcomes and translation are restricted by several drawbacks, such as low drug loading, premature drug leakage and carrier-related toxicity.

**Abbreviations:** ABC, accelerated blood clearance; ACT, adoptive cell transfer; ATP, adenosine triphosphate; ATO, atovaquone;  $\alpha$ -PD-L1, anti-PD-L1 monoclonal antibody; BV, Biliverdin; Ber, berberine; Ce6, chlorin e6; CTLs, cytotoxic T lymphocytes; CPT, camptothecin; CI, combination index; DOX, doxorubicin; dsRNA, double-stranded RNA; DPDNAs, dual pure drug nano-assemblies; DBNP, DOX-Ber nano-assemblies; DBNP@CM, DBNP were cloaked with 4T1 cell membranes; DCs, dendritic cells; EPR, enhanced permeability and retention; EGFR, epithelial growth factor receptor; EPI, epirubicin; FRET, Forster Resonance Energy Transfer; GEF, gefitinib; HCPT, hydroxycamptothecin; HMGB1, high-mobility group box 1; ICG, indocyanine green; IC<sub>50</sub>, half maximal inhibitory concentration; ICD, immunogenic cell death; ICB, immunologic checkpoint blockade; ITM, immunosuppressive tumor microenvironment; MPDNAs, multiple pure drug nano-assemblies; MTX, methotrexate; MDS, molecular dynamics simulations; MRI, magnetic resonance imaging; Nano-DDSs, nanoparticulate drug delivery systems; NIR, near-infrared; NSCLC, non-small cell lung cancer; NPs, nanoparticles; PDNAs, pure drug nano-assemblies; PTX, paclitaxel; PPa, pheophorbide A; PAI, photoacoustic imaging; PTT, photothermal therapy; PDT, photodynamic therapy; PD-1, PD receptor 1; PD-L1, PD receptor 1 ligand; Poly I:C, polyriboinosinic:polyribocytidylic acid; QSNAP, quantitative structure-nanoparticle assembly prediction; RNA, ribonucleic acid; RBC, red blood cell; ROS, reactive oxygen species; SPDNAs, single pure drug nano-assemblies; TME, tumor microenvironment; TEM, transmission electron microscopy; TTT, trastuzumab; Top I & II, topoisomerase I & II; TLR4, Toll-like receptor 4; TNBC, triple negative breast; TA, tannic acid; UA, ursolic acid; YSV, tripeptide tyroservatide; ZHO, Z-Histidine-Obzl.

\*Corresponding author.

E-mail address: [yingleizhai@syphu.edu.cn](mailto:yingleizhai@syphu.edu.cn) (Yinglei Zhai).

<sup>†</sup>These authors made equal contributions to this work.

Peer review under responsibility of Chinese Pharmaceutical Association and Institute of Materia Medica, Chinese Academy of Medical Sciences.

<https://doi.org/10.1016/j.apsb.2021.08.012>

2211-3835 © 2022 Chinese Pharmaceutical Association and Institute of Materia Medica, Chinese Academy of Medical Sciences. Production and hosting by Elsevier B.V. This is an open access article under the CC BY-NC-ND license (<http://creativecommons.org/licenses/by-nc-nd/4.0/>).

Carrier-free;  
Self-assembly;  
Combination therapy;  
Cancer treatment;  
Pure drug;  
Nanomedicine

Recently, pure drug nano-assemblies (PDNAs), fabricated by the self-assembly or co-assembly of pure drug molecules, have attracted considerable attention. Their facile and reproducible preparation technique helps to remove the bottleneck of nanomedicines including quality control, scale-up production and clinical translation. Acting as both carriers and cargos, the carrier-free PDNAs have an ultra-high or even 100% drug loading. In addition, combination therapies based on PDNAs could possibly address the most intractable problems in cancer treatment, such as tumor metastasis and drug resistance. In the present review, the latest development of PDNAs for cancer treatment is overviewed. First, PDNAs are classified according to the composition of drug molecules, and the assembly mechanisms are discussed. Furthermore, the co-delivery of PDNAs for combination therapies is summarized, with special focus on the improvement of therapeutic outcomes. Finally, future prospects and challenges of PDNAs for efficient cancer therapy are spotlighted.

© 2022 Chinese Pharmaceutical Association and Institute of Materia Medica, Chinese Academy of Medical Sciences. Production and hosting by Elsevier B.V. This is an open access article under the CC BY-NC-ND license (<http://creativecommons.org/licenses/by-nc-nd/4.0/>).

## 1. Introduction

Cancer is always a global health threaten to human beings<sup>1</sup>. Through the fight with cancer in the past decades, various approaches have been built for cancer treatment, including surgery, drug therapy and biotherapy<sup>2–4</sup>. Conventionally, surgery removal remains the preferred approach for localized tumors<sup>5</sup>. However, for those metastatic tumors, the limitation of surgery is obvious because of the widespread metastatic lesions<sup>6,7</sup>. Therefore, drug therapies, which could work systemically in both solid tumors and distant metastases, have played an irreplaceable role in cancer treatment<sup>8,9</sup>. The anticancer drugs now comprise of chemotherapeutic drugs, photosensitizers and immunomodulatory molecules<sup>10,11</sup>. Unfortunately, the clinical outcomes of the anticancer drugs are far from satisfactory, possibly owing to the quick clearance, narrow therapeutic window, inefficient tumor accumulation and serious off-target toxicity<sup>12</sup>. In response, drug delivery technologies are highlighted for efficient cancer drug therapy.

Encouragingly, nanoparticulate drug delivery systems (Nano-DDSs) have emerged as potent solution to the obstacles of anticancer drug delivery<sup>13,14</sup>. The nanosized particles exhibit distinct advantages including: (i) improving the solubility and chemical stability of the packaged drugs; (ii) prolonging the blood circulation time of the drugs; (iii) increasing the cellular uptake efficacy; (iv) targeting drug delivery to tumor sites by the well-known enhanced permeability and retention (EPR) effect or grafting targeting ligands<sup>15</sup>. However, most Nano-DDSs usually encapsulate the drugs in carrier materials through intermolecular interactions, such as hydrophobic interactions<sup>16</sup>. The drugs may lack of affinity with the carrier materials, leading to premature drug leakage<sup>17</sup>. In addition, the overused carrier materials limit the drug loading efficiency (usually less than 10%) and might bring the carrier-related toxicity<sup>18–20</sup>. Furthermore, despite the advances of some novel Nano-DDS, their preparation techniques could be too laborious for clinical translation<sup>21</sup>. Rational design of advanced Nano-DDSs remains challenging.

Recently, pure drug nano-assemblies (PDNAs), fabricated by the self-assembly or co-assembly of pure drug molecules, have attracted considerable attention. Drug molecules without any chemical modification could spontaneously form uniform nanoparticles (NPs), usually by the one-step nanoprecipitation method<sup>22,23</sup>. This is different from the traditional nanocrystal preparations, obtained by pearl milling, high pressure homogenization, etc.<sup>24</sup>. The facile and reproducible nanoprecipitation

method could help to remove the bottleneck of nanomedicines including quality control, scale-up produce and clinical translation. None or only a small amount of surfactants are needed to improve the colloidal stability of PDNAs<sup>25</sup>. Acting as both carriers and cargos, the carrier-free PDNAs have an ultra-high drug loading (more than 60% or even 100%). Besides, the co-assembly behavior of PDNAs could availably co-deliver dual or multi drug for combination therapies, which is conducive to address the most intractable problems in cancer treatment, such as tumor metastasis and drug resistance<sup>26,27</sup>. PDNAs have been widely used for the combinations of tumor diagnosis, chemotherapy, phototherapy and immunotherapy. The emerging PDNAs are in urgent need to be well summarized and reviewed.

In the present review, the latest development of PDNAs for cancer treatment is outlined (Fig. 1). First, PDNAs are classified according to the composition of drug molecules, and the corresponding assembly mechanisms are discussed. Furthermore, we focus on the co-delivery of PDNAs for combination therapies and the excellent therapeutic outcomes. Finally, challenges and future prospects of PDNAs for efficient cancer therapy are spotlighted.

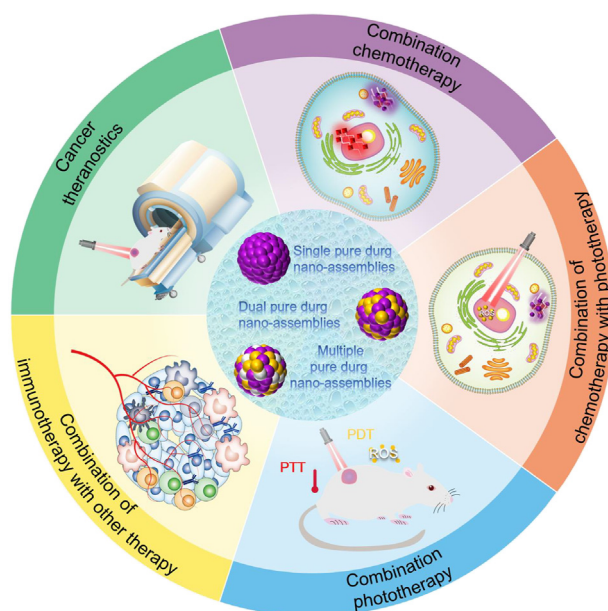


**Figure 1** Pure drug nano-assemblies for efficient cancer therapy.

## 2. Nano-assembly of pure drug molecules

PDNAs are intended to consist entirely of active drug molecules, without inactive molecules or chemicals. Depending on the composition of drug modules, PDNAs could be divided into three types: (i) single pure drug nano-assemblies (SPDNAs), which are self-assembled by single kind of drug modules; (ii) dual pure drug nano-assemblies (DPDNAs), which are co-assembled from dual kinds of drugs, and (iii) multiple pure drug nano-assemblies (MPDNAs), which are formed by the co-assembly of more than two kinds of drugs. The assembly of the drug modules is mainly driven by the noncovalent bond interactions, including hydrophobic interactions, intermolecular  $\pi$ - $\pi$  stacking, hydrogen bonding, and electrostatic forces, etc. For some amphiphilic molecules, the hydrophilic groups could be exposed on the surface of the NPs, during the assembly process, to achieve 100% drug loading (*e.g.*, irinotecan-SN38 nano-assemblies)<sup>28</sup>. As for hydrophobic molecules, due to the high surface free energy, a small amount of surfactants may be added to improve the colloidal stability<sup>22,25</sup>. The developed PDNAs for cancer therapy are summarized in Table 1<sup>22,23,25,28-61</sup>. In this section, the three types of PDNAs will be introduced and we will take an insight into the assembly mechanisms of PDNAs.

### 2.1. Self-assembly of pure single drug

In aqueous solution, drug molecules would dissolve or precipitate into large aggregates. Interestingly, some drug molecules would spontaneously self-assemble into SPDNAs. For instance, DiR molecules could form uniform nano-assemblies using the simple one-step nanoprecipitation method (Fig. 2A)<sup>22</sup>. The addition of surfactant (DSPE-PEG2k, 20%, w/w) significantly improved the colloid stability of DiR nano-assemblies. Compared with DiR solution and DiR nano-assemblies, PEGylated DiR nano-assemblies had distinct therapeutic advantages in terms of cellular uptake efficacy and pharmacokinetic profiles, leading to the improved tumor accumulation. Therefore, PEGylated DiR nano-assemblies demonstrated strong photothermal antitumor activity. However, most antineoplastic drug molecules do not have a good self-assembly capability and special preparation methods were required such as precisely controlled temperature, suitable concentration, and ultrasound treatment, etc.<sup>29,30</sup>. Even so, oversized spherical or rod-shaped particles may be possibly obtained due to the excessive crystallization<sup>30,31</sup>.

In addition to finding the “proper” self-assembling molecules, another approach to construct SPDNAs is to utilize “proper” preparation methods. Different from the traditional methods, a novel ice-template assisted strategy was invented<sup>32</sup>. The detailed technical scheme was shown in Fig. 2B. A unique property of ice is that its grain boundaries contain relatively mobile water molecules behaving like liquid<sup>62-64</sup>. Therefore, the ice template was equivalent to a special aqueous solution. The ice-template-assisted strategy could apply to a series of drug molecules, including: curcumin, camptothecin, paclitaxel, 6-mercaptopurine, squaraine, methotrexate, teniposide and some of their derivatives. By simply adjusting the processing parameters, nano-assemblies with different sizes (~20–200 nm) could be controllably obtained. This novel approach had major advantages over the traditional nanoprecipitation method in mass production, size tunability, production costs and application range.

### 2.2. Co-assembly of dual drugs

The co-assembly of two different drug molecules could be described as an equilibrium of the intermolecular interactions between the two molecules. Compared with SPDNAs, DPDNAs showed distinct advantages in terms of the assembly capability. For example, single paclitaxel (PTX) self-assembled into unstable nanorods NPs with a length of  $254.7 \pm 119$  nm and a width of  $76.5 \pm 21$  nm<sup>30</sup>. In contrast, the co-assemblies of PTX and indocyanine green (ICG) were stable nanospheres (diameter:  $112 \pm 1.06$  nm, PDI: 0.1)<sup>33</sup>. The similar example was the SPDNAs of hydroxycamptothecin (HCPT) and the DPDNAs of HCPT and doxorubicin (DOX)<sup>34-36</sup>. The ratio of the two molecules could also affect the morphology and stability of the nano-assemblies. It is known that HCPT alone would form large needle-shaped NPs in water<sup>37</sup>. When using ICG to co-assemble with HCPT, as the ratio of ICG increased, the ICG-HCPT nano-assemblies gradually shaped nice nanospheres (Fig. 3A<sub>2</sub>)<sup>37</sup>. Finally, the molar ratio of 2:1 (HCPT to ICG) was found to form nano-assemblies with smallest particle size and PDI. Besides, red blood cell (RBC) membranes could be cloaked onto the surface of ICG-HCPT nano-assemblies to increase the biocompatibility and blood circulation time (Fig. 3A<sub>1</sub>).

As we know, the tumor microenvironment (TME) is quite different from normal tissues, as a result of the uncontrollable tumor growth and metastasis<sup>65-67</sup>. One ubiquitous characteristic is the dysregulated pH value (pH 5.5–7.0) than normal tissues (pH 7.4)<sup>68,69</sup>. In some cases of DPDNAs, tumor-specific pH-responsiveness could be achieved dependent upon the structure of the drug molecules. For example, irinotecan-curcumin nano-assemblies showed tunable surface charges from  $-10$  mV in normal physiological condition to  $+40$  mV under the TME (Fig. 3B)<sup>38</sup>. This negative to positive charge conversion improved the tumor cellular uptake of the NPs. It was also reported that less than 20% of HCPT was released from the HCPT-ICG co-assemblies at pH 7.4 in 10 h, whereas the percentage increased to 80% at pH 5.5<sup>37</sup>. Even after RBC membranes coating, more HCPT could still be released at low pH condition.

Apart from the common nanospheres and nanorods, PDNAs could also take the form of nanofibers. In a recent study, porphyrin and adenosine triphosphate (ATP) were co-assembled into supra-molecular helical nanofibers<sup>39</sup>. As it is known, ATP is negatively charged<sup>70</sup>. The cationic molecules interacted with the planar  $\pi$ -systems of porphyrin through electrostatic interactions, leading to the formation of the unique nanofibers. Notably, ATP could be hydrolyzed by the over-expressed phosphatase enzymes in tumor sites to facilitate the controllable release. Furthermore, the ATP concentration in tumor sites is hundreds of times higher than that in normal tissues<sup>71,72</sup>. The overexpressed ATP could stabilize the porphyrin-ATP from premature de-assembly. In addition, as we know the NPs are generally internalized by tumor cells *via* the ATP-dependent endocytosis<sup>73,74</sup>, therefore the endogenous ATP coupled with the delivered extracellular ATP could further facilitate the cellular uptake of the nanofibers.

### 2.3. Co-assembly of multiple drugs

The co-assembly of multiple drugs could be more intricate than dual drugs because more drug molecules should reach an equilibrium of intermolecular interactions. There have been reports of

**Table 1** List of pure drug nano-assemblies for cancer therapy.

| Drug 1                 | Drug 2                  | Drug 3              | Ratio <sup>a</sup>    | Drug loading | Ref.     |
|------------------------|-------------------------|---------------------|-----------------------|--------------|----------|
| Curcumin               | —                       | —                   | —                     | 78%          | 25       |
|                        | —                       | —                   | —                     | 100%         | 32       |
| Ursolic acid           | —                       | —                   | —                     | ~60%         | 29       |
| DiR                    | —                       | —                   | —                     | 80%          | 22       |
| Camptothecin           | —                       | —                   | —                     | 74.8%        | 31       |
|                        | —                       | —                   | —                     | 100%         | 32       |
| Hydroxycamptothecin    | —                       | —                   | —                     | 78%          | 36       |
| Paclitaxel             | —                       | —                   | —                     | 88.5%        | 30       |
|                        | —                       | —                   | —                     | 100%         | 32       |
| Doxorubicin            | —                       | —                   | —                     | 90.47%       | 46       |
| Chlorin e6             | —                       | —                   | —                     | 100%         | 47       |
| BMS-202                | —                       | —                   | —                     | 100%         | 47       |
| Vitamin B <sub>2</sub> | —                       | —                   | —                     | —            | 48       |
| Teniposide             | —                       | —                   | —                     | 100%         | 32       |
| Squaraine              | —                       | —                   | —                     | 100%         | 32       |
| Methotrexate           | —                       | —                   | —                     | 100%         | 32       |
| H2TpyP                 | —                       | —                   | —                     | 100%         | 32       |
| 6-mercaptopurine       | —                       | —                   | —                     | 100%         | 32       |
| Teniposide             | Paclitaxel              | —                   | —                     | 100%         | 32       |
|                        | H2TpyP                  | —                   | —                     | 100%         | 32       |
| Ursolic acid           | Isothiocyanate          | —                   | —                     | —            | 29       |
| Hydroxycamptothecin    | Doxorubicin             | —                   | 1:4 (m)               | ~100%        | 28,34,35 |
| Irinotecan             | SN38                    | —                   | 1:1 (m)               | ~100%        | 38       |
|                        | Curcumin                | —                   | 1:2 (m)               | ~95%         | 38       |
| Topotecan              | Curcumin                | —                   | —                     | —            | 49       |
| Clopidogrel            | Pheophorbide A          | —                   | 37.1:29 (w)           | 66.1%        | 50       |
| Indocyanine green      | Epirubicin              | —                   | 1:2 (m)               | ~92%         | 37       |
|                        | Hydroxycamptothecin     | —                   | 1:2 (m)               | ~92%         | 33       |
|                        | Paclitaxel              | —                   | 9.2:90.7 (w)          | ~100%        | 33       |
|                        | NLG919                  | —                   | —                     | —            | 33       |
|                        | Gefitinib               | —                   | —                     | —            | 33       |
|                        | Sorafenib               | —                   | —                     | —            | 33       |
|                        | Vandetanib              | —                   | —                     | —            | 33       |
|                        | Probuco                 | —                   | —                     | —            | 33       |
|                        | Bicalutamide            | —                   | —                     | —            | 33       |
|                        | Celecoxib               | —                   | —                     | —            | 33,51    |
|                        | Azelnidipine            | —                   | —                     | —            | 45       |
| Chlorin e6             | Sorafenib               | —                   | 1:1 (w)               | ~100%        | 52       |
|                        | Doxorubicin             | —                   | 2:1 (m)               | ~100%        | 53       |
|                        | Hydroxycamptothecin     | —                   | 1:4 (m)               | —            | 53       |
|                        | Fmoc-L-Lys              | —                   | 1:4 (w)               | ~100%        | 54       |
|                        | Diphenylalanine         | —                   | 1:4 (w)               | ~100%        | 55       |
|                        | Erastin                 | —                   | 1:3.55 (w)            | ~100%        | 47       |
|                        | Atovaquone              | —                   | 26.7:73.3 (w)         | ~100%        | 23       |
|                        | BMS-202                 | —                   | 1:2 (w)               | 100%         | 23       |
| DiR                    | Chlorin e6              | —                   | 2:1 (m)               | 100%         | 23       |
|                        | Hypericin               | —                   | 2:1 (m)               | 100%         | 23       |
|                        | 3-Bodipy-propanoic acid | —                   | 2:1 (m)               | 100%         | 23       |
|                        | Zinc phthalocyanine     | —                   | 2:1 (m)               | 100%         | 56       |
|                        | Pheophorbide A          | —                   | 2:1 (m)               | 100%         | 57       |
| Paclitaxel             | Indomethacin            | —                   | 1:2 (w)               | —            | 58       |
|                        | Poly I:C                | —                   | 64:3 (w)              | 67%          | 39       |
| Gefitinib              | Tyroservatide           | —                   | 1:11.25 (w)           | ~100%        | 59       |
| Porphyrin              | Adenosine triphosphate  | —                   | ~6:4 (w)              | ~100%        | 60       |
| Doxorubicin            | Celastrol               | Mn <sup>2+</sup>    | 1:4 (m)               | ~100%        | 61       |
|                        | Berberine               | Trastuzumab         | 4:1 (w)               | —            | 40       |
| Biliverdin             | Z-Histidine-Obzl        | Methotrexate        | 6:2:5 (m)             | ~100%        | 41       |
| Camptothecin           | Doxorubicin             | H <sub>2</sub> TPyP | 25.7:67.3:7 (w)       | ~100%        | 43       |
| Hydroxycamptothecin    | Paclitaxel              | Ursolic acid        | 49.1:26.6:24.3 (w)    | —            | 42       |
| Curcumin               | Perylene                | Doxorubicin         | 77.6:22.3:0.1 (w)     | ~100%        | 44       |
| Indocyanine green      | Paclitaxel              | —                   | 23.58:51.27:25.14 (w) | ~100%        | —        |
|                        | Tannic acid             | —                   | ~37:39:24 (w)         | ~100%        | —        |

—Not applicable.

<sup>a</sup>The molar ratio is abbreviated as (m), and the mass ratio was abbreviated as (w).

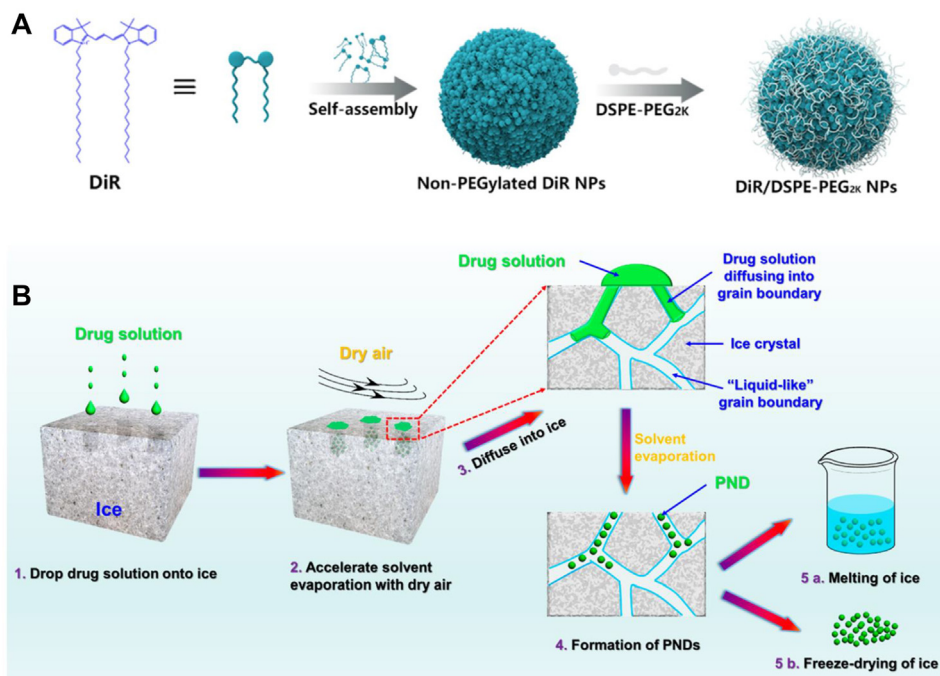


**Figure 2** (A) Self-assembly of DiR molecules into uniform nano-assemblies. Reprinted with the permission from Ref. 22. Copyright © 2018 ACS Publishing Group. (B) Schematic illustration of the ice-template-assisted strategy. Reprinted with the permission from Ref. 32. Copyright © 2018 ACS Publishing Group.

MPDNAs such as camptothecin (CPT)-trastuzumab (TTZ)-DOX, PTX-HCPT-methotrexate (MTX), PTX-ICG-ursolic acid (UA), perylene-curcumin-H2TPyP, etc.<sup>40–43</sup>. It is noticeable that MPDNAs usually contains a self-assembling molecule, or a co-assembling molecule pair (*e.g.*, CPT-DOX, ICG-PTX)<sup>33,35</sup>. Therefore, considering the different affinity between drug molecules, Xiong et al.<sup>44</sup> reported a step-by-step assembling method. Firstly, DOX and tannic acid (TA) were mixed and co-assembled to form DT NPs *via*  $\pi$ - $\pi$  stacking and electrostatic interactions (Fig. 4A). Thereafter, ICG was added in the system to further co-assembled with DT NPs. Apart from  $\pi$ - $\pi$  stacking and electrostatic interactions, the hydroxyl group of DOX provided lone pair electrons to interact with  $N^+$  of ICG, which induced the  $n$ - $\pi^*$  transition and led to the formation of the final DTIG NPs (Fig. 4B). What is worth mentioning is that all three components of DTIG NPs are water-soluble, and the whole preparation process avoided the use of organic solvents. Taking advantage of the reversible proton concentration changes of TA, DTIG NPs showed special hydrophilic-hydrophobic conversion and size conversion capabilities (Fig. 4C). In the TME (pH 6.5), DTIG NPs could transformed into hydrophobic NPs to increase the cellular uptake efficiency. Subsequently, in the lysosomes (pH 4.5), the particle size of DTIG NPs could greatly swell to nearly 1.5  $\mu$ m to rupture the lysosomes. After the lysosome escape and entering the cytoplasm, the oversized DTIG NPs could quickly redissolve and recover to normal sizes ( $152.7 \pm 1.9$  nm).

#### 2.4. Insight into the assembly mechanisms of pure drug nano-assemblies

The functional groups in the chemical structure of anticancer drug molecules induce the intermolecular interactions between drug molecules or drug and water molecules. For example, aromatic groups could induce  $\pi$ - $\pi$  stackings; aliphatic groups lead to

hydrophobic interactions; ionic groups have electrostatic forces; hydroxyl or carboxyl group interacts *via* hydrogen bonding, and so on<sup>75–79</sup>. Usually, in aqueous solution, the anticancer drugs either aggregate into precipitation (aggregation, the forces between drugs dominate) or dissolve into solution (non-aggregation, the forces between drug and water dominate, Fig. 5A)<sup>80,81</sup>. PDNAs exist in the form of colloid in aqueous solution, that is, the two trends just reach a proper equilibrium (Fig. 5B). Such as DiR molecules, the aromatic heads could provide strong  $\pi$ - $\pi$  stacking forces for aggregation, while the long aliphatic tails could introduce steric hindrance in case of the over-aggregation into precipitation<sup>22</sup>. However, the self-assembly of single drug is relatively difficult. For example, although UA could be self-assembled, further ultrasonic processing was required<sup>29</sup>.

In the case of co-assembly, the assembly could be easier with the help of other molecules to balance the intermolecular interactions (Fig. 5C). Hydrophilic drugs (*e.g.*, DOX and ICG) need to increase the trend of aggregation, while hydrophobic drugs (*e.g.*, PTX and HCPT) need to reduce the trend of aggregation<sup>33,34,44</sup>. It is not difficult to perceive that photosensitizers, such as ICG, chlorine e6 (Ce6), and pheophorbide A (PPa), could provide good co-assembly capability<sup>23,33,45</sup>. In a work, ICG was used as a template to co-assemble with a series of anticancer drugs including PTX, NLG919, gefitinib, sorafenib, vandetanib, probucol, bicalutamide, celecoxib and azelnidipine<sup>33</sup>. This is possibly owing to the conjugate structures of photosensitizers, which could produce strong  $\pi$ - $\pi$  stacking interactions between molecules<sup>82,83</sup>. Because of the strong  $\pi$ - $\pi$  stacking, the different drug molecules could have a good affinity and dock with each other by edge-to-face, offset or face-to-surface stacking to form aggregates simultaneously<sup>84,85</sup>.

A major dilemma for PDNAs is that the assembly process is hardly to predict, execute and control. The searching for PDNAs is still through empirical or experimental screening. Fortunately,

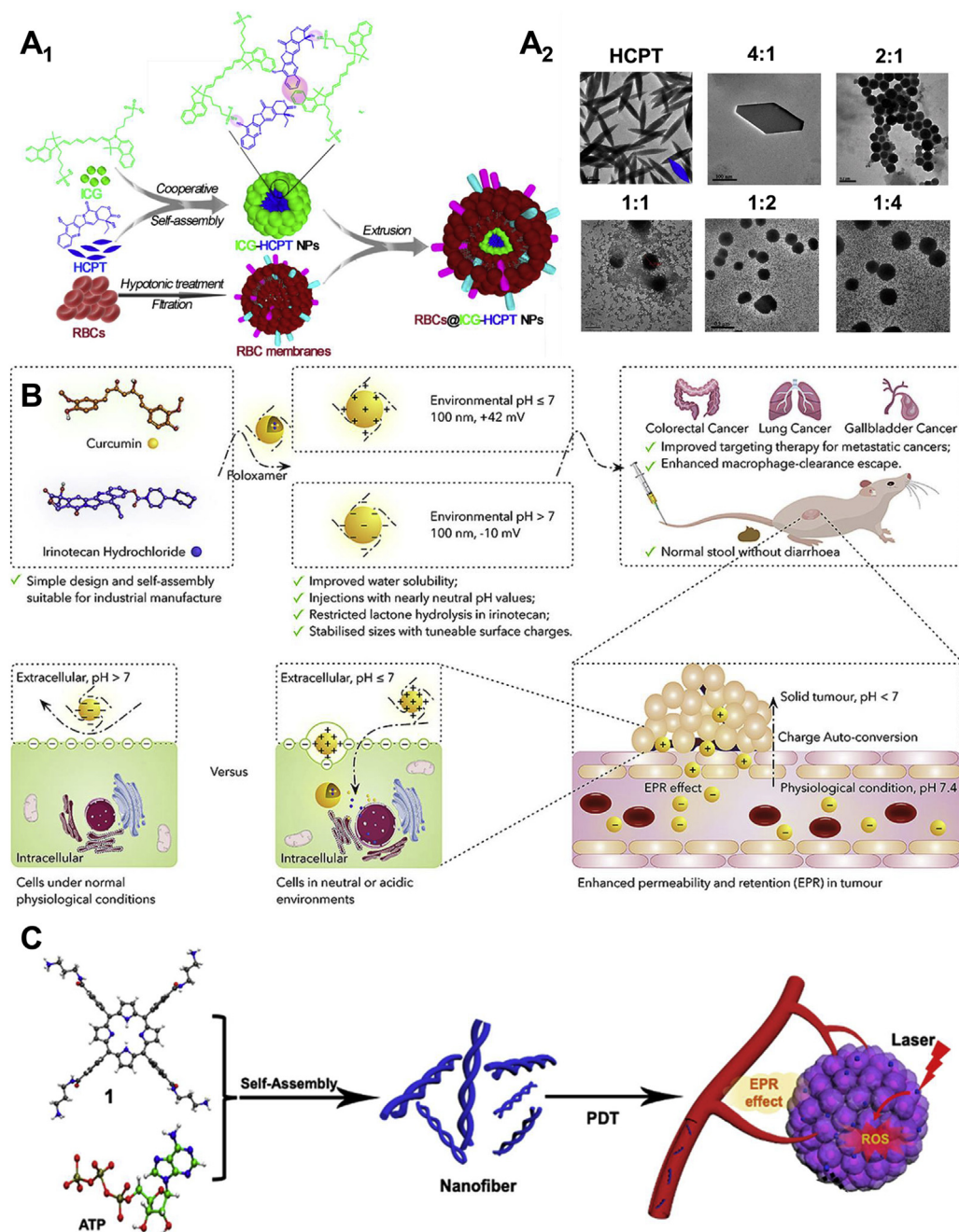


**Figure 3** (A<sub>1</sub>) Schematic illustration of the RBC membranes cloaked ICG-HCPT nano-assemblies. (A<sub>2</sub>) Transmission electron microscopy (TEM) images of ICG-HCPT nano-assemblies with different molar ratios of HCPT to ICG (1:0, 4:1, 2:1, 1:1, 1:2, and 1:4). Reprinted with the permission from Ref. 37. Copyright © 2019 ACS Publishing Group. (B) Schematic illustration of the charge-conversional irinotecan-curcumin nano-assemblies for better targeted cancer therapy. Reprinted with the permission from Ref. 38. Copyright © 2020 Elsevier Inc. (C) Schematic illustration of the porphyrin-ATP nanofibers. Reprinted with the permission from Ref. 39. Copyright © 2021 ACS Publishing Group.

with the development of computer science, molecular dynamics simulations (MDS) have been applied as a novel approach to investigate the intermolecular interactions<sup>86–88</sup>. A quantitative structure-nanoparticle assembly prediction (QSNAP) model was proposed<sup>89</sup>. Using indocyanine dyes to co-assemble with a series of hydrophobic drugs, the nano-assembly formulation and the particle size could be accurately predicted by QSNAP. Although the scope of such technology has yet to be widened, we still look forward to the emergence of a wild-applicable technic that could rationally predict and optimize PDNAs in the future.

### 3. Efficient combination cancer therapy based on pure drug nano-assemblies

Cancer is a complex adaptive system. Long-term use of one single drug could easily produce the phenomenon of drug resistance and lose therapeutic efficacy<sup>90–92</sup>. Therefore, in both preclinical studies and clinical applications, combination therapy has indicated enhanced efficacy than mono therapy because it targets different key pathways synergistically or additively<sup>93,94</sup>. The combined approach could potentially reduce adverse effect, reverse multi drug resistance, prevent

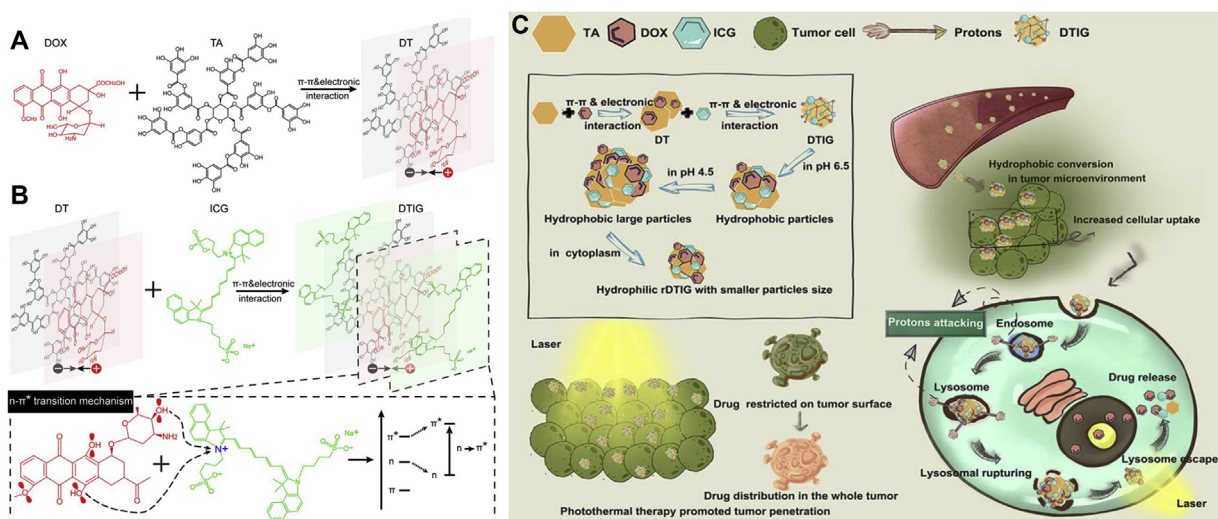


**Figure 4** Step-by-step assembly process and lysosome escape of DTIG NPs. (A) First step assembly of DOX and TA into DT NPs. (B) Second step assembly of ICG and DT NPs into DTIG NPs. (C) Schematic illustration of the hydrophilic-hydrophobic conversion and size conversion of DTIG NPs. Reprinted with the permission from Ref. 44. Copyright © 2020 ACS Publishing Group.

tumor metastasis and relapse<sup>83,95,96</sup>. Benefited by the special co-assembly capability, PDNAs could sufficiently co-deliver drug molecules for various combinations of tumor diagnosis, chemotherapy, phototherapy and immunotherapy. The possible combinations based on PDNAs have highlighted the anti-tumor advantages<sup>7,97,98</sup>. In this section, we will focus on the combination therapies based on PDNAs, with focus on the enhancement of therapeutic effects.

### 3.1. Cancer theranostics

Theranostics Nano-DDSs could not only deliver therapeutic agents to targeting lesions, but also detect the *in vivo* destiny of the

NPs<sup>99,100</sup>. In cancer treatment, a rationally designed Nano-DDSs could help to reduce the off-target toxicity and improve the drug-delivery efficiency for precision medicine<sup>101,102</sup>. Xing and coworkers<sup>61</sup> developed a multimodal theranostics nanoplatform integrating both photoacoustic imaging (PAI), magnetic resonance imaging (MRI) and photothermal therapy (PTT) into one system (Fig. 6A). Biliverdin (BV) was chosen as photosensitizer for PTT and PAI agent for tumor diagnosis with high spatial resolution and penetration depth. Of note, BV was derived from heme catabolism and could be rapidly metabolized to bilirubin for bile and urine excretion, thereby exhibiting good biocompatibility<sup>103,104</sup>. In addition, Z-Histidine-Obzl (ZHO), a metal-binding short peptide,

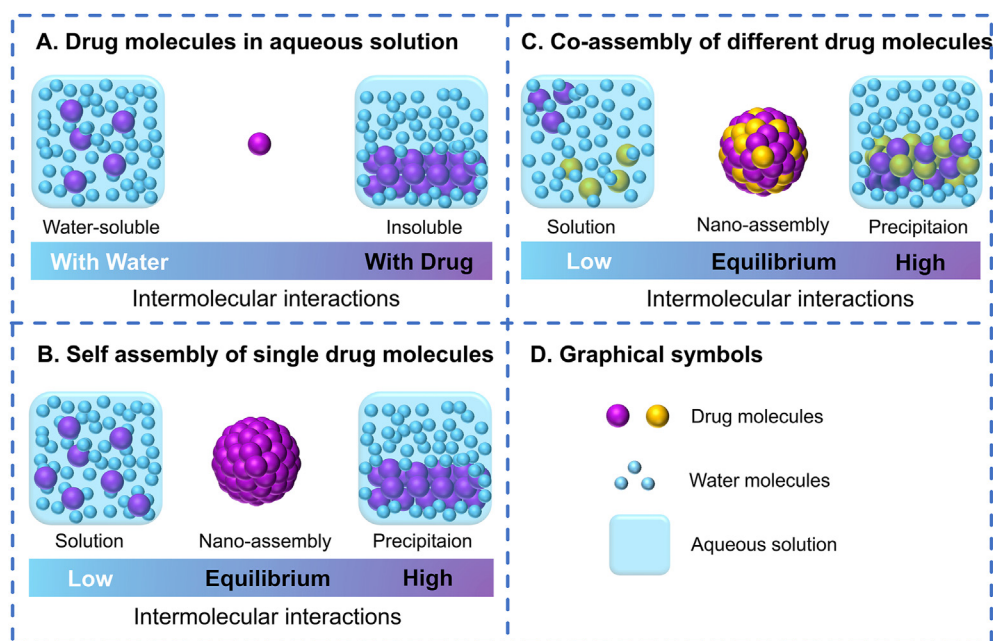


**Figure 5** Assembly mechanisms of pure drug nano-assemblies. (A) Intermolecular interactions between drug molecules and water molecules in aqueous solution. (B) Intermolecular interactions during the self-assembly of single drug molecules in aqueous solution. (C) Intermolecular interactions during the co-assembly of different drug molecules in aqueous solution. (D) Graphical symbols.

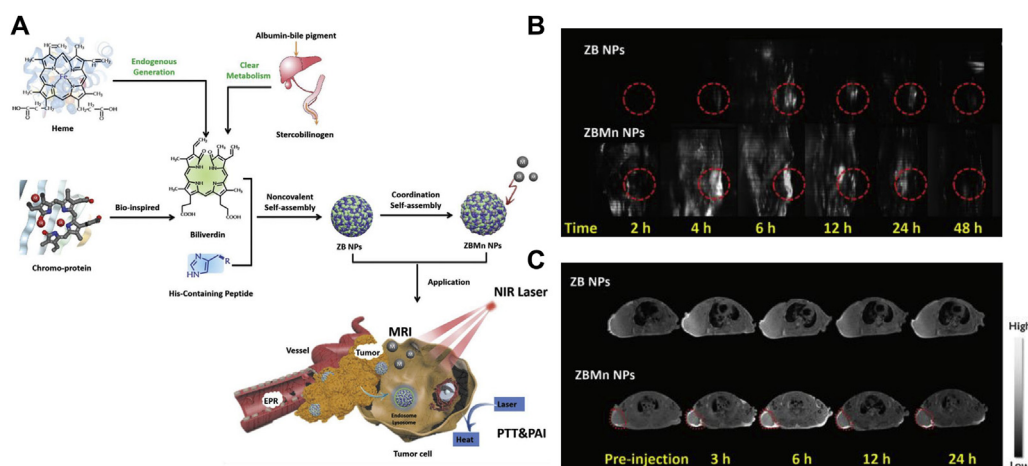


**Figure 6** BVMn NPs for multimodal tumor imaging and photothermal therapy. (A) Schematic illustration of BVMn NPs. (B) Photoacoustic imaging of MCF-7 tumor-bearing mice treated with BVMn NPs. (C)  $T_1$ -weighted magnetic resonance imaging of MCF-7 tumor-bearing mice treated with BVMn NPs. Reprinted with the permission from Ref. 61. Copyright © 2019 John Wiley and Sons Group.

was utilized to bind  $Mn^{+}$  for MRI. BV and ZHO could co-assemble into ZB NPs, and further coordinated  $Mn^{+}$  to form ZBMn NPs. From the PAI and MRI imagines (Fig. 6B and C), the maximum accumulation of both ZB and ZBMn NPs was found to be 6 h post administration. Therefore, a wave of near-infrared (NIR) laser was treated 6 h post administration for PTT. Finally, ZBMn NPs successfully ablated human breast tumors with no recurrence during the 24 days of observation.

### 3.2. Combination chemotherapy

Chemotherapy is still the mainstay of cancer therapy<sup>105,106</sup>. However, the efficacy of chemotherapy is restricted by the severe side effects and multidrug resistance<sup>107–109</sup>. Combination chemotherapy using two or multiple chemotherapeutics, which kills cancerous cells *via* different working sites or mechanisms, holds the promise to solve the obstacles<sup>110,111</sup>. For example, HCPT inhibits the activity of a topoisomerase I (top I) enzyme to induce DNA damage, and DOX intercalates between DNA base pairs and inhibits topoisomerase II (top II) enzyme to interference with DNA synthesis<sup>112,113</sup>. As reported, the top I inhibitor could reverse the drug resistant of top II resistant cells. Therefore, DOX-HCPT nano-assemblies showed potent proliferation inhibition of MCF-7R multidrug resistant cells<sup>34</sup>. Besides, gefitinib (GEF) was co-assembled with tripeptide tyroservatide (YSV) to construct GEF-YSV nano-assemblies<sup>58</sup>. GEF could inhibit epithelial growth factor receptor (EGFR) to induce the apoptosis of cancer cells, and YSV could interrupt the cell cycles and suppress the activity of histone deacetylase<sup>114,115</sup>. Both GEF and YSV were highly selective to tumor cells, and showed low toxicity against normal cells. Finally, GEF-YSV nano-assemblies effectively prohibited the growth of non-small cell lung cancer (NSCLC) without additional toxicity burden.

A paradox of chemotherapy is that not only does it control tumors, it may also promote tumor progression<sup>116,117</sup>. For example, DOX-exacerbated breast cancer metastasis was reported to correlate with the activation of toll-like receptor 4 (TLR4), which is triggered by high-mobility group box 1 (HMGB1)<sup>118,119</sup>. Berberine (Ber), an anticancer alkaloid, has been demonstrated as an HMGB1-TLR4 axis regulator<sup>120</sup>. In response, DOX-Ber nano-assemblies (DBNP) were developed for defeating chemotherapy-exacerbated breast cancer metastasis (Fig. 7A)<sup>60</sup>. In addition, DBNP were cloaked with 4T1 cell membranes (DBNP@CM).

Compared with DBNP, DBNP@CM displayed much higher tumor accumulation efficiency (Fig. 7B), benefiting from the homing effect. As a result, DBNP@CM showed favorable inhibition of tumor growth and even metastasis (Fig. 7C).

In addition to the combination of dual chemotherapeutics, Barua and Mitragotri<sup>40</sup> designed CPT-TTZ-DOX nano-assemblies for triple chemotherapy. When the CPT-TTZ-DOX NPs were internalized into tumor cells, monoclonal antibody TTZ was recycled to the plasma membranes, leaving CPT in the perinuclear region and delivering DOX into the nucleus. The three drugs respectively worked on their targeting sites, and had a great synergistic effect with a combination index (CI) of  $0.17 \pm 0.03$  on BT-474 cells. The half maximal inhibitory concentration ( $IC_{50}$ ) of CPT-TTZ-DOX NPs was 10–10000-fold lower than that of individual drugs. Besides, TTZ, CPT and DOX would arrest cells in the G0/G1, S, or G2/M phases, respectively<sup>121–124</sup>. The co-delivery of CPT-TTZ-DOX NPs significantly reversed the cell cycle arrest, compared with single TTZ and TTZ-CPT NPs.

### 3.3. Combination phototherapy

Phototherapy, including photodynamic therapy (PDT) and PTT, is a promising non-invasive approach for cancer treatment<sup>125</sup>. PTT raises the local temperature to promote cell necrosis, and PDT produces reactive oxygen species (ROS) to induce cell apoptosis<sup>126,127</sup>. One hindrance of the clinical translation of phototherapy is the severe phototoxicity<sup>128</sup>. The patients treated with phototherapy have to avoid the exposure to light before the complete excretion of photosensitizers<sup>129</sup>. For better therapeutic effect and lower side effect, a Forster Resonance Energy Transfer (FRET) photosensitizer pairs was co-assembled for cascade-activatable PTT/PDT (Fig. 8A)<sup>23</sup>. Ce6 was chosen as FRET donor and DiR served as FRET acceptor. In the nano-assemblies of Ce6@DiR, Ce6 could be quenched by DiR by the FRET interaction, the photosensitivity of which was thus “turned off”. Only when DiR was first photobleached by 808 nm laser, the PDT of Ce6 would be “turned on”. Moreover, erythrocyte camouflaged coating (Ce6@DiR-M NPs) was utilized to improve the pharmacokinetic behaviors. Compared with Ce6@DiR NPs and Ce6@DiR-PEG NPs (PEGylated), Ce6@DiR-M NPs not only had the longest blood circulation time, but also avoided the accelerated



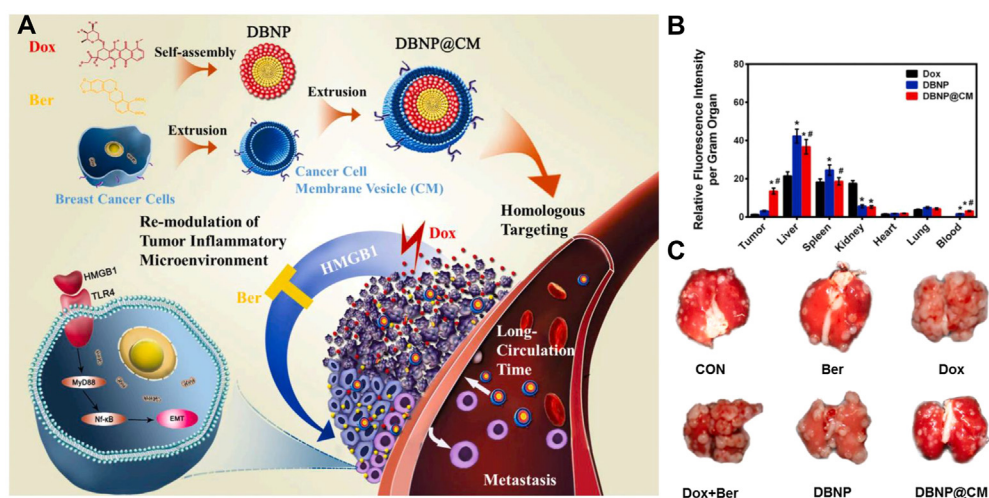


**Figure 7** (A) Schematic illustration of DBNP@CM for efficient chemotherapy with minimal chemotherapy-exacerbated metastasis. (B) Biodistribution of DBNP@CM. (C) Images of lung tissues. Reprinted with the permission from Ref. 60. Copyright © 2021, Elsevier Inc.

blood clearance (ABC) effect of the PEGylation formulation. The advantage could be attributed to the immune escape of erythrocyte camouflage, which expressed the “don’t eat me” marker CD47<sup>130</sup>. Overall, the proliferation of triple negative breast cancer (TNBC) was significantly inhibited by Ce6@DiR-M NPs.

### 3.4. Combination of chemotherapy with phototherapy

Phototherapy has shown a promising synergy with chemotherapy in terms of therapeutic outcomes for cancer treatment<sup>131–133</sup>. In response, a series of PDNAs were developed for chemotherapy in combination with PTT or PDT<sup>42,52,54</sup>. For instance, Li and co-workers<sup>50</sup> developed epirubicin (EPI)-ICG nano-assemblies for chemo-photothermal synergistic therapy. On one hand, ICG-induced PTT could ablate tumors by cell necrosis. The temperature in tumor sites of ICG-EPI NPs treated group could reach as

high as 53.9 °C, much higher than that of 37.5 °C of free ICG group. As a result, the tumor permeability was increased, thereby facilitating the deep penetration of the NPs. On the other hand, the released EPI exerted cytotoxicity to kill tumor cells. Eventually, the EPI-ICG NPs magically eradicated TNBC without recurrence during the 21 days of treatment cycle, whereas chemotherapy or PTT alone could not completely cure tumors.

As for PDT, photosensitizers could efficiently generate reactive oxygen species (ROS), such as singlet oxygen (<sup>1</sup>O<sub>2</sub>), which could damage DNA and induce apoptosis<sup>134,135</sup>. Therefore, the combination of PDT and DNA damage drugs always led to good synergies (e.g., Ce6-DOX nano-assemblies and Ce6-HCPT nano-assemblies)<sup>45,52</sup>. However, it is well known that photodynamic therapy (PDT) requires the consumption of O<sub>2</sub> to produce ROS, and it does not work well in hypoxic tumors<sup>136,137</sup>. To solve the dilemma, Ce6 was co-assembled with an oxidative phosphorylation inhibitor

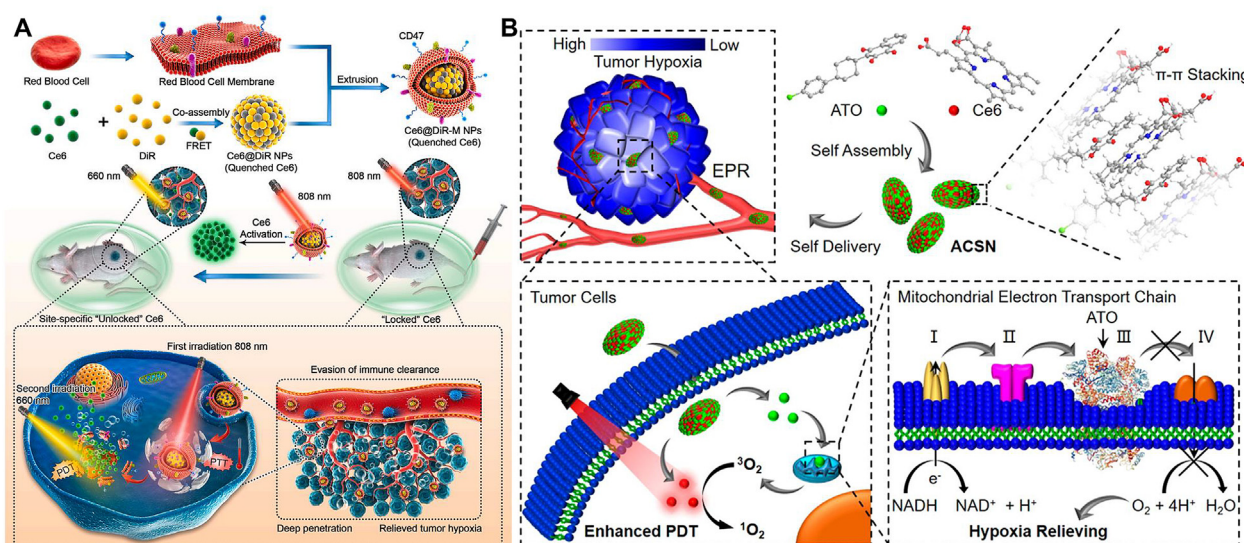


**Figure 8** (A) Schematic illustration of the FRET photosensitizer pairs co-assembled erythrocyte camouflaged Ce6@DiR-M NPs for programmed cascade-activatable PTT-PDT with low phototoxicity. Reprinted with the permission from Ref. 23. Copyright © 2021 Elsevier Inc. (B) Schematic illustration of ATO-Ce6 NPs for O<sub>2</sub>-economized PDT. Reprinted with the permission from Ref. 55. Copyright © 2020 ACS Publishing Group.

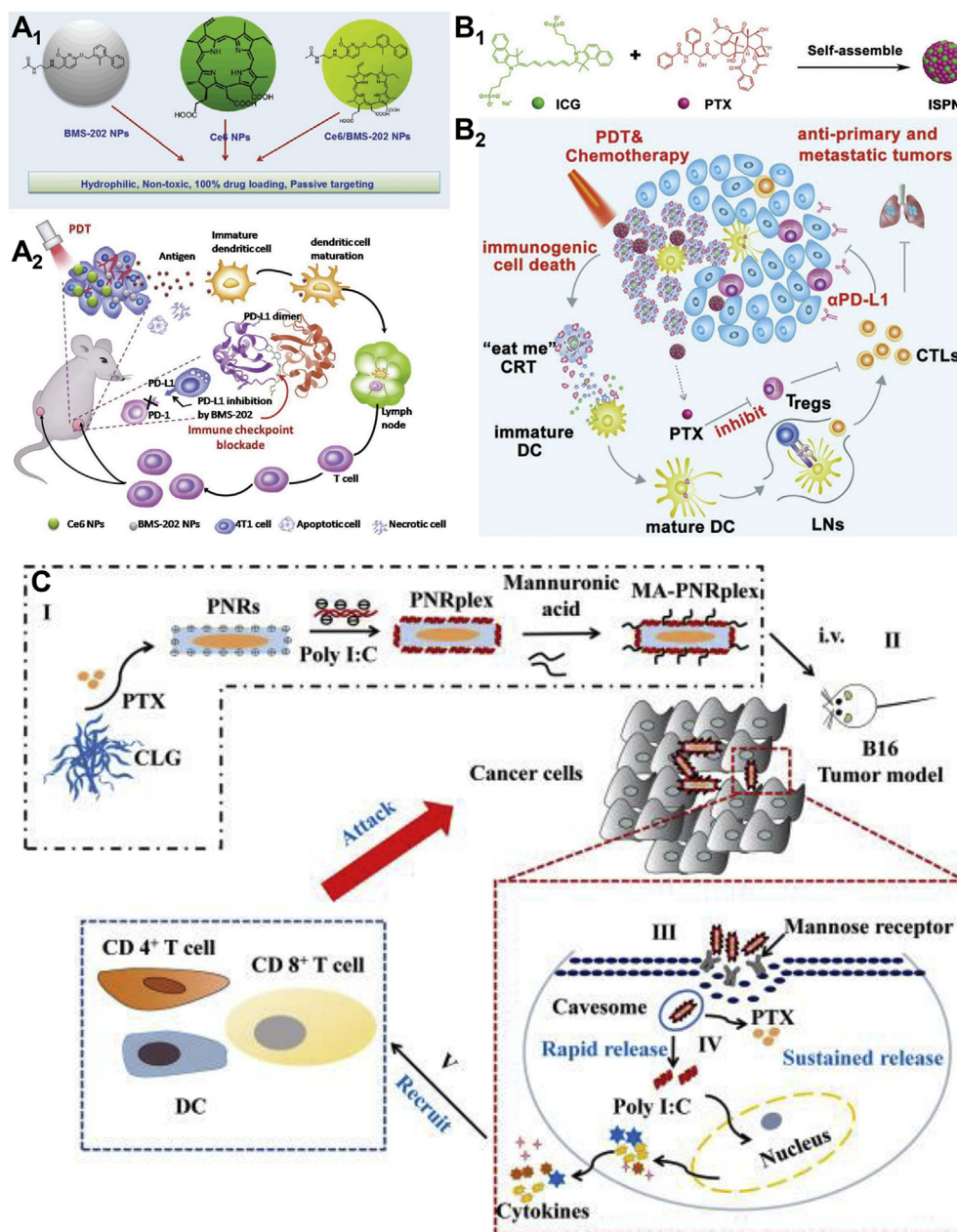


**Figure 9** (A<sub>1</sub>) Molecular presentation and self-assembly of Ce6 and BMS-202. (A<sub>2</sub>) Ce6/BMS-202 NPs potentiate PD-L1 blockade to induce systemic antitumor immunity for combination of ICB immunotherapy and PDT. Reprinted with the permission from Ref. 47. Copyright © 2019 John Wiley and Sons Group. (B<sub>1</sub>) Self-assembly of PTX-ICG nano-assemblies. (B<sub>2</sub>) Schematic illustration of PTX-ICG NPs for immuno-photochemo triple therapy. Reprinted with the permission from Ref. 33. Copyright © 2020 John Wiley and Sons Group. (C) Schematic illustration of the PNRplex for cytosolic targeting chemo-immunotherapy. Reprinted with the permission from Ref. 57. Copyright © 2021 Elsevier Inc.

(atovaquone, ATO) for O<sub>2</sub>-economized PDT against hypoxic tumors (Fig. 8B)<sup>55</sup>. As a mitochondrial complex III inhibitor, ATO interrupted the electron transport chain pathway and suppressed the activity of oxidative phosphorylation to decrease O<sub>2</sub> consumption. The relieved hypoxia TME could in turn improved efficiency of PDT. After the treatment of ATO-Ce6 NPs, the majority of 4T1 tumors vanished, highlighting the superiority of the O<sub>2</sub>-economized PDT.

### 3.5. Combination of immunotherapy with other therapy

In the past decades, tumor immunotherapy has emerged and revolutionized cancer treatment<sup>138,139</sup>. The use of cytokine or

checkpoint inhibitors, cancer vaccines or adoptive cell transfer (ACT) therapy strengthens or normalizes (suppresses or activates) the immune system of patients to inhibit tumors<sup>140,141</sup>. Immunotherapy is not only proved effective for primary tumors, but also prevents tumor metastasis and relapse of tumors<sup>142,143</sup>. The commonly used immunomodulatory molecules include small molecule drugs and antibody drugs<sup>141,144,145</sup>. Among them, some small molecule drugs could be rationally formulated into PDNAs.

Immunologic checkpoint blockade (ICB) immunotherapy is one of the most profound and successful immunotherapies in clinic, among which the most well-known pathway is the anti-programmed cell death (anti-PD) pathway, including PD receptor

1 (PD-1) and PD receptor 1 ligand (PD-L1)<sup>9,146,147</sup>. BMS-202 is a small molecule PD-1 inhibitor, which withstands the dimerization of PD-L1 protein, thereby preventing the formation of PD-1/PD-L1 complex<sup>148</sup>. BMS-202 could already self-assemble into uniform NPs (Fig. 9A<sub>1</sub>)<sup>47</sup>. Besides, it could further co-assemble with Ce6 to form Ce6/BMS-202 NPs. It was found that BMS-202 NPs alone could increase the maturation of dendritic cells (DCs) and infiltration of antigen-specific T cells into 4T1 tumors as well as anti-PD-L1 monoclonal antibody ( $\alpha$ -PD-L1) (Fig. 9A<sub>2</sub>). Combined with ICB and PDT, Ce6/BMS-202 NPs significantly suppressed the growth of primary and distant tumors, owing to the augmentative immune cells such as CD8<sup>+</sup> T cells, matured DCs, and memory T cells. The results revealed that small molecule PD-1 inhibitors have the same clinical value as  $\alpha$ -PD-L1.

Despite the advances of ICB therapy, the therapeutic performance could be limited by the immunosuppressive tumor micro-environment (ITM)<sup>149–151</sup>. Apart from novel immunomodulatory molecules, traditional chemotherapeutics were also startlingly able to reverse the ITM to benefit ICB therapy<sup>152–154</sup>. For instance, a low dose of PTX could reduce the intratumorally infiltrating regulatory T cells (T<sub>regs</sub>) and suppress the T<sub>regs</sub>-related immune inhibitory<sup>155,156</sup>. In addition, PDT could induce immunogenic cell death (ICD)<sup>157,158</sup>. The combination of ICB therapy with chemotherapy or PDT could further facilitate the intratumoral infiltration of cytotoxic T lymphocytes (CTLs) and overcome the ITM<sup>159–161</sup>. In response, PTX-ICG nano-assemblies were devised for immuno-photo-chemo triple therapy (Fig. 9B<sub>1</sub> and B<sub>2</sub>)<sup>33</sup>. The PTX-ICG NPs had good colloidal stability and could be lyophilized for long-time storage. Accompanied with  $\alpha$ -PD-L1 treatment, PTX-ICG NPs efficiently suppressed TNBC and tumor relapse by promoting the intratumoral infiltration of CTLs through PDT-induced ICD and inhibiting the recruitment of T<sub>regs</sub> to relieve ITM.

Gene-based immunotherapy have been widely concerned due to the potent efficacy and little toxicity<sup>162,163</sup>. Ribonucleic acid (RNA), as one of the most important genetic molecules, showed great potential in the construction of anti-cancer drugs and cancer vaccines<sup>164,165</sup>. To illustrate, Du and coworkers<sup>57</sup> designed a drug-delivering-drug system for the co-delivery of PTX and poly-riboinosinic:polyribocytidylic acid (Poly I:C) that is a safe synthetic analog of double-stranded RNA (dsRNA)<sup>166</sup>. Using a simple antisolvent-precipitation method, Poly I:C were coated on the self-assembled PTX nanorods. To further target mannose-receptor, D-mannuronic acids were used for final surface modification to form the PNR/Poly I:C complex (PNRplex) (Fig. 9C). The rod-shaped PNRplex were internalized into tumor cells *via* the caveolin-mediated endocytosis, thereby avoiding the enzyme breakdown in the endo-lysosomes and targeting cytoplasm<sup>74,167</sup>. Inside the cytoplasm, PTX induced the apoptosis of tumor cells and Poly I:C upregulated interferons, chemokines and inflammatory cytokines. Overall, the PNRplex markedly amplified the immune response including the maturation of DCs and the infiltration of CD4<sup>+</sup> T cells and CD8<sup>+</sup> T cells for the potent chemo-immunotherapy.

#### 4. Conclusions

In this review, we overviewed the latest development of PDNAs. First, according to the composition of the drugs, PDNAs were classified and the assembly mechanisms were discussed. Afterwards, the combination therapies based on PDNAs were summarized with focus on the enhanced therapeutic outcomes. Herein, challenges and future prospects of PDNAs for efficient cancer therapy are outlined.

#### 4.1. Challenges

PDNAs have shown the potentiality for efficient anticancer drug delivery. However, for their successful clinical application, there are still a multitude of problems to be solved. First, the determination of whether a molecule could be self-assembled or co-assembled still depends on empirical deduction or experimental screening. The self-assembly and co-assembly of PDNAs are generally governed by the equilibrium of the intermolecular forces. This process is difficult to observe and analyze. Fortunately, with the development of computer sciences, MDS have been built as a forecasting tool for elucidating the assembly of PDNAs. At present, MDS are still mostly used for validation, not prediction. The emergence of QSNAP is a chance, but there is still a long path to go before it becomes a utility tool. Furthermore, the optimization of PDNAs has usually pursued the finest formulation of NPs (considering particle size, PDI and colloidal stability). Under this circumstance, for DPNAs and MPDNAs, the finest formulation could hardly be the best synergistic ratio between the drugs. How to exert the best synergistic effect of PDNAs remains challenging. Last but not least, there are still many concerns about the translational studies and the gap between animal studies and human beings. In the scale-up production, will the particle size and PDI of PDNAs remain uniform? As PDNAs are mainly administered by intravenous injection, could PDNAs be sterilized without failure? What are the real pharmacokinetic behaviors and *in vivo* destiny of PDNAs in the human body? These problems as well as the self-assembly and synergistic effect of PDNAs are the future research highlights of PDNAs.

#### 4.2. Future prospects

In response to the unsatisfactory performance of simple anticancer drugs and traditional Nano-DDS, the carrier-free PDNAs have emerged as a facile nanoplatform for efficient cancer therapy. PDNAs are a widely applicable nanoplatform, featured with both functional modification and translational potential. PDNAs have been widely used for mono therapy, and the combinations of tumor diagnosis, chemotherapy, phototherapy and immunotherapy. Their advantages including facile and reproducible preparation technique, ultra-high drug loading and efficient co-delivery behavior, demonstrate a promising nanomedicine for clinical oncology. The era of cancer immunotechnology has arrived. The progress of PDNAs in immunotherapy is also pretty eye-catching. With more research on PDNAs and parse on the assembly mechanisms, we believe that there will be clinical trials and even medical products of PDNAs in the near future.

#### Acknowledgments

This work was supported by Liaoning Science & Technology project (2019-ZD-0465, China).

#### Author contributions

Shuwen Fu and Guanting Li mainly wrote the manuscript and contributed equally to the manuscript. Wenli Zang provided suggestions for the improvement of manuscript. Xinyu Zhou and Kexin Shi contributed to the correction of the manuscript. Yinglei Zhai contributed to the conception of the study and helped perform the analysis with constructive discussions.

## Conflicts of interest

The authors declare no conflicts of interest.

## References

- Sung H, Ferlay J, Siegel RL, Laversanne M, Soerjomataram I, Jemal A, et al. Global cancer statistics 2020: GLOBOCAN estimates of incidence and mortality worldwide for 36 cancers in 185 countries. *CA Cancer J Clin* 2021;**3**:209–49.
- Neoptolemos JP, Kleeff J, Michl P, Costello E, Greenhalf W, Palmer DH. Therapeutic developments in pancreatic cancer: current and future perspectives. *Nat Rev Gastroenterol Hepatol* 2018;**15**:333–48.
- Sawyers C. Targeted cancer therapy. *Nature* 2004;**432**:294–7.
- Yun SH, Kwok SJ. Light in diagnosis, therapy and surgery. *Nat Biomed Eng* 2017;**1**:1–16.
- Si Y, Yuan P, Hu N, Wang X, Ju J, Wang J, et al. Primary tumor surgery for patients with *de novo* stage IV breast cancer can decrease local symptoms and improve quality of life. *Ann Surg Oncol* 2020;**27**:1025–33.
- Alieva M, van Rheenen J, Broekman ML. Potential impact of invasive surgical procedures on primary tumor growth and metastasis. *Clin Exp Metastasis* 2018;**35**:319–31.
- Yang F, Zhao Z, Sun B, Chen Q, Sun J, He Z, et al. Nanotherapeutics for antimetastatic treatment. *Trends Canc* 2020;**6**:645–59.
- Sun B, Luo C, Cui W, Sun J, He Z. Chemotherapy agent-unsaturated fatty acid prodrugs and prodrug-nanoplatforams for cancer chemotherapy. *J Control Release* 2017;**264**:145–59.
- Zugazagoitia J, Guedes C, Ponce S, Ferrer I, Molina-Pinelo S, Paz-Ares L. Current challenges in cancer treatment. *Clin Ther* 2016;**38**:1551–66.
- Hait WN. Anticancer drug development: the grand challenges. *Nat Rev Drug Discov* 2010;**9**:253–4.
- Zhou X, Liu X, Huang L. Macrophage-mediated tumor cell phagocytosis: opportunity for nanomedicine intervention. *Adv Funct Mater* 2021;**31**:2006220.
- Luo C, Sun J, Sun B, He Z. Prodrug-based nanoparticulate drug delivery strategies for cancer therapy. *Trends Pharmacol Sci* 2014;**35**:556–66.
- Sato Y, Nakamura T, Yamada Y, Harashima H. The nanomedicine rush: new strategies for unmet medical needs based on innovative nano DDS. *J Control Release* 2020;**330**:305–16.
- Brannon-Peppas L, Blanchette JO. Nanoparticle and targeted systems for cancer therapy. *Adv Drug Deliv Rev* 2004;**56**:1649–59.
- Peer D, Karp JM, Hong S, Farokhzad OC, Margalit R, Langer R. Nanocarriers as an emerging platform for cancer therapy. *Nat Nanotechnol* 2007;**2**:751–60.
- Zhao Y, Fay F, Hak S, Perez-Aguilar JM, Sanchez-Gaytan BL, Goode B, et al. Augmenting drug-carrier compatibility improves tumour nanotherapy efficacy. *Nat Commun* 2016;**7**:1–11.
- Dai J, Lin S, Cheng D, Zou S, Shuai X. Interlayer-crosslinked micelle with partially hydrated core showing reduction and pH dual sensitivity for pinpointed intracellular drug release. *Angew Chem Int Ed* 2011;**50**:9404–8.
- Cai K, He X, Song Z, Yin Q, Zhang Y, Uckun FM, et al. Dimeric drug polymeric nanoparticles with exceptionally high drug loading and quantitative loading efficiency. *J Am Chem Soc* 2015;**137**:3458–61.
- Yang Y, Sun B, Zuo S, Li X, Zhou S, Li L, et al. Trisulfide bond-mediated doxorubicin dimeric prodrug nanoassemblies with high drug loading, high self-assembly stability, and high tumor selectivity. *Sci Adv* 2020;**6**:eabc1725.
- Su C, Liu Y, Li R, Wu W, Fawcett JP, Gu J. Absorption, distribution, metabolism and excretion of the biomaterials used in nanocarrier drug delivery systems. *Adv Drug Deliv Rev* 2019;**143**:97–114.
- Min Y, Caster JM, Eblan MJ, Wang AZ. Clinical translation of nanomedicine. *Chem Rev* 2015;**115**:11147–90.
- Zhang X, Sun B, Zuo S, Chen Q, Gao Y, Zhao H, et al. Self-assembly of a pure photosensitizer as a versatile theragnostic nanoplatforam for imaging-guided antitumor photothermal therapy. *ACS Appl Mater Interfaces* 2018;**10**:30155–62.
- Zhang X, Xiong J, Wang K, Yu H, Sun B, Ye H, et al. Erythrocyte membrane-camouflaged carrier-free nanoassembly of FRET photosensitizer pairs with high therapeutic efficiency and high security for programmed cancer synergistic phototherapy. *Bioact Mater* 2021;**6**:2291–302.
- Müller RH, Gohla S, Keck CM. State of the art of nanocrystals—special features, production, nanotoxicology aspects and intracellular delivery. *Eur J Pharm Biopharm* 2011;**78**:1–9.
- Zhang J, Li S, An FF, Liu J, Jin S, Zhang JC, et al. Self-carried curcumin nanoparticles for *in vitro* and *in vivo* cancer therapy with real-time monitoring of drug release. *Nanoscale* 2015;**7**:13503–10.
- Vasan N, Baselga J, Hyman DM. A view on drug resistance in cancer. *Nature* 2019;**575**:299–309.
- Kosharsky B, Solban N, Chang SK, Rizvi I, Chang Y, Hasan T. A mechanism-based combination therapy reduces local tumor growth and metastasis in an orthotopic model of prostate cancer. *Cancer Res* 2006;**66**:10953–8.
- Hu S, Lee E, Wang C, Wang J, Zhou Z, Li Y, et al. Amphiphilic drugs as surfactants to fabricate excipient-free stable nanodispersions of hydrophobic drugs for cancer chemotherapy. *J Control Release* 2015;**220**:175–9.
- Fan L, Zhang B, Xu A, Shen Z, Guo Y, Zhao R, et al. Carrier-free, pure nanodrug formed by the self-assembly of an anticancer drug for cancer immune therapy. *Mol Pharm* 2018;**15**:2466–78.
- Park J, Sun B, Yeo Y. Albumin-coated nanocrystals for carrier-free delivery of paclitaxel. *J Control Release* 2017;**263**:90–101.
- Guo F, Fan Z, Yang J, Li Y, Wang Y, Zhao H, et al. A comparative evaluation of hydroxycamptothecin drug nanorods with and without methotrexate prodrug functionalization for drug delivery. *Nanoscale Res Lett* 2016;**11**:1–7.
- Zhang J, Nie W, Chen R, Chelora J, Wan Y, Cui X, et al. Green mass production of pure nanodrugs via an ice-template-assisted strategy. *Nano Lett* 2018;**19**:658–65.
- Feng B, Niu Z, Hou B, Zhou L, Li Y, Yu H. Enhancing triple negative breast cancer immunotherapy by ICG-templated self-assembly of paclitaxel nanoparticles. *Adv Funct Mater* 2020;**30**:1906605.
- Zhao Y, Chen F, Pan Y, Li Z, Xue X, Okeke CI, et al. Nanodrug formed by coassembly of dual anticancer drugs to inhibit cancer cell drug resistance. *ACS Appl Mater Interfaces* 2015;**7**:19295–305.
- Chen F, Zhao Y, Pan Y, Xue X, Zhang X, Kumar A, et al. Synergistically enhanced therapeutic effect of a carrier-free HCPT/DOX nanodrug on breast cancer cells through improved cellular drug accumulation. *Mol Pharm* 2015;**12**:2237–44.
- Li W, Yang Y, Wang C, Liu Z, Zhang X, An F, et al. Carrier-free, functionalized drug nanoparticles for targeted drug delivery. *Chem Commun* 2012;**48**:8120–2.
- Ye S, Wang F, Fan Z, Zhu Q, Tian H, Zhang Y, et al. Light/pH-triggered biomimetic red blood cell membranes camouflaged small molecular drug assemblies for imaging-guided combinational chemo-photothermal therapy. *ACS Appl Mater Interfaces* 2019;**11**:15262–75.
- Xiao H, Guo Y, Liu H, Liu Y, Wang Y, Li C, et al. Structure-based design of charge-conversional drug self-delivery systems for better targeted cancer therapy. *Biomaterials* 2020;**232**:119701.
- Li Z, Li S, Guo Y, Yuan C, Yan X, Schanze KS. Metal-free nanoassemblies of water-soluble photosensitizer and adenosine triphosphate for efficient and precise photodynamic cancer therapy. *ACS Nano* 2021;**15**:4979–88.
- Barua S, Mitragotri S. Synergistic targeting of cell membrane, cytoplasm, and nucleus of cancer cells using rod-shaped nanoparticles. *ACS Nano* 2013;**7**:9558–70.

41. Zhou M, Zhang X, Yang Y, Liu Z, Tian B, Jie J, et al. Carrier-free functionalized multidrug nanorods for synergistic cancer therapy. *Biomaterials* 2013;**34**:8960–7.
42. Guo Y, Jiang K, Shen Z, Zheng G, Fan L, Zhao R, et al. A small molecule nanodrug by self-assembly of dual anticancer drugs and photosensitizer for synergistic near-infrared cancer theranostics. *ACS Appl Mater Interfaces* 2017;**9**:43508–19.
43. Zhang J, Liang Y-C, Lin X, Zhu X, Yan L, Li S, et al. Self-monitoring and self-delivery of photosensitizer-doped nanoparticles for highly effective combination cancer therapy *in vitro* and *in vivo*. *ACS Nano* 2015;**9**:9741–56.
44. Xiong H, Wang Z, Wang C, Yao J. Transforming complexity to simplicity: protein-like nanotransformer for improving tumor drug delivery programmatically. *Nano Lett* 2020;**20**:1781–90.
45. Zhang R, Xing R, Jiao T, Ma K, Chen C, Ma G, et al. Carrier-free, chemophotodynamic dual nanodrugs via self-assembly for synergistic antitumor therapy. *ACS Appl Mater Interfaces* 2016;**8**:13262–9.
46. Yu C, Zhou M, Zhang X, Wei W, Chen X, Zhang X. Smart doxorubicin nanoparticles with high drug payload for enhanced chemotherapy against drug resistance and cancer diagnosis. *Nanoscale* 2015;**7**:5683–90.
47. Zhang R, Zhu Z, Lv H, Li F, Sun S, Li J, et al. Immune checkpoint blockade mediated by a small-molecule nanoinhibitor targeting the PD-1/PD-L1 pathway synergizes with photodynamic therapy to elicit antitumor immunity and antimetastatic effects on breast cancer. *Small* 2019;**15**:1903881.
48. Fei J, Dai L, Gao F, Zhao J, Li J. Assembled vitamin B2 nanocrystals with optical waveguiding and photosensitizing properties for potential biomedical application. *Angew Chem Int Ed* 2019;**58**:7254–8.
49. Wang Q, Sun M, Li D, Li C, Luo C, Wang Z, et al. Cytochrome P450 enzyme-mediated auto-enhanced photodynamic cancer therapy of co-nanoassembly between clopidogrel and photosensitizer. *Theranostics* 2020;**10**:5550.
50. Li Y, Liu G, Ma J, Lin J, Lin H, Su G, et al. Chemotherapeutic drug-photothermal agent co-self-assembling nanoparticles for near-infrared fluorescence and photoacoustic dual-modal imaging-guided chemo-photothermal synergistic therapy. *J Control Release* 2017;**258**:95–107.
51. Wei Z, Liang P, Xie J, Song C, Tang C, Wang Y, et al. Carrier-free nano-integrated strategy for synergetic cancer anti-angiogenic therapy and phototherapy. *Chem Sci* 2019;**10**:2778–84.
52. Wen Y, Zhang W, Gong N, Wang YF, Guo H-B, Guo W, et al. Carrier-free, self-assembled pure drug nanorods composed of 10-hydroxycamptothecin and chlorin e6 for combinatorial chemophotodynamic antitumor therapy *in vivo*. *Nanoscale* 2017;**9**:14347–56.
53. Liu K, Xing R, Zou Q, Ma G, Möhwald H, Yan X. Simple peptide-tuned self-assembly of photosensitizers towards anticancer photodynamic therapy. *Angew Chem* 2016;**128**:3088–91.
54. Zhu T, Shi L, Yu C, Dong Y, Qiu F, Shen L, et al. Ferroptosis promotes photodynamic therapy: supramolecular photosensitizer-inducer nanodrug for enhanced cancer treatment. *Theranostics* 2019;**9**:3293.
55. Zhao LP, Zheng RR, Chen HQ, Liu LS, Zhao XY, Liu HH, et al. Self-delivery nanomedicine for O<sub>2</sub>-economized photodynamic tumor therapy. *Nano Lett* 2020;**20**:2062–71.
56. Zhang C, Long L, Xiong Y, Wang C, Peng C, Yuan Y, et al. Facile engineering of indomethacin-induced paclitaxel nanocrystal aggregates as carrier-free nanomedicine with improved synergistic antitumor activity. *ACS Appl Mater Interfaces* 2019;**11**:9872–83.
57. Du X, Hou Y, Huang J, Pang Y, Ruan C, Wu W, et al. Cytosolic delivery of the immunological adjuvant Poly I:C and cytotoxic drug crystals via a carrier-free strategy significantly amplifies immune response. *Acta Pharm Sin B* 2021;**11**:3272–85.
58. Zhang Z, Shi L, Wu C, Su Y, Qian J, Deng H, et al. Construction of a supramolecular drug–drug delivery system for non-small-cell lung cancer therapy. *ACS Appl Mater Interfaces* 2017;**9**:29505–14.
59. Xiao Y, Liu J, Guo M, Zhou H, Jin J, Liu J, et al. Synergistic combination chemotherapy using carrier-free celastrol and doxorubicin nanocrystals for overcoming drug resistance. *Nanoscale* 2018;**10**:12639–49.
60. Zheng X, Zhao Y, Jia Y, Shao D, Zhang F, Sun M, et al. Biomimetic co-assembled nanodrug of doxorubicin and berberine suppresses chemotherapy-exacerbated breast cancer metastasis. *Biomaterials* 2021:120716.
61. Xing R, Zou Q, Yuan C, Zhao L, Chang R, Yan X. Self-assembling endogenous biliverdin as a versatile near-infrared photothermal nanoagent for cancer theranostics. *Adv Mater* 2019;**31**:1900822.
62. Schulson EM. The structure and mechanical behavior of ice. *JOM* 1999;**51**:21–7.
63. Di Prinzio C, Nasello O. Study of grain boundary motion in ice bicrystals. *J Phys Chem B* 1997;**101**:7687–90.
64. Canale L, Comtet J, Nigues A, Cohen C, Clanet C, Siria A, et al. Nanorheology of interfacial water during ice gliding. *Phys Rev X* 2019;**9**:041025.
65. Mbeunkui F, Johann DJ. Cancer and the tumor microenvironment: a review of an essential relationship. *Cancer Chemother Pharmacol* 2009;**63**:571–82.
66. Thakkar S, Sharma D, Kalia K, Tekade RK. Tumor microenvironment targeted nanotherapeutics for cancer therapy and diagnosis: a review. *Acta Biomater* 2020;**101**:43–68.
67. Tao W, He Z. ROS-responsive drug delivery systems for biomedical applications. *Asian J Pharm Sci* 2018;**13**:101–12.
68. Lee ES, Gao Z, Bae YH. Recent progress in tumor pH targeting nanotechnology. *J Control Release* 2008;**132**:164–70.
69. Gao W, Chan JM, Farokhzad OC. pH-Responsive nanoparticles for drug delivery. *Mol Pharm* 2010;**7**:1913–20.
70. Dhiman S, Jain A, Kumar M, George SJ. Adenosine-phosphate-fueled, temporally programmed supramolecular polymers with multiple transient states. *J Am Chem Soc* 2017;**139**:16568–75.
71. Okuro K, Sasaki M, Aida T. Boronic acid-appended molecular glues for ATP-responsive activity modulation of enzymes. *J Am Chem Soc* 2016;**138**:5527–30.
72. Di Virgilio F, Adinolfi E. Extracellular purines, purinergic receptors and tumor growth. *Oncogene* 2017;**36**:293–303.
73. Sahay G, Alakhova DY, Kabanov AV. Endocytosis of nanomedicines. *J Control Release* 2010;**145**:182–95.
74. Iversen T-G, Skotland T, Sandvig K. Endocytosis and intracellular transport of nanoparticles: present knowledge and need for future studies. *Nano Today* 2011;**6**:176–85.
75. Claessens CG, Stoddart JF.  $\pi$ - $\pi$  interactions in self-assembly. *J Phys Org Chem* 1997;**10**:254–72.
76. Niu D, Jiang Y, Ji L, Ouyang G, Liu M. Self-assembly through co-ordination and  $\pi$ -stacking: controlled switching of circularly polarized luminescence. *Angew Chem Int Ed* 2019;**58**:5946–50.
77. Chandler D. Interfaces and the driving force of hydrophobic assembly. *Nature* 2005;**437**:640–7.
78. Sastry M, Rao M, Ganesh KN. Electrostatic assembly of nanoparticles and biomacromolecules. *Acc Chem Res* 2002;**35**:847–55.
79. Sherrington DC, Taskinen KA. Self-assembly in synthetic macromolecular systems via multiple hydrogen bonding interactions. *Chem Soc Rev* 2001;**30**:83–93.
80. Endres TK, Beck-Broichsitter M, Samsonova O, Renette T, Kissel TH. Self-assembled biodegradable amphiphilic PEG–PCL–IPEI triblock copolymers at the borderline between micelles and nanoparticles designed for drug and gene delivery. *Biomaterials* 2011;**32**:7721–31.
81. Siepmann J, Siepmann F. Mathematical modeling of drug dissolution. *Int J Pharm* 2013;**453**:12–24.
82. Shi Y, Elkhazab A, Yousef Yengej FA, van den Dikkenberg J, Hennink WE, van Nostrum CF.  $\pi$ - $\pi$  stacking induced enhanced

- molecular solubilization, singlet oxygen production, and retention of a photosensitizer loaded in thermosensitive polymeric micelles. *Adv Healthc Mater* 2014;**3**:2023–31.
83. Wang M, Zhai Y, Ye H, Lv Q, Sun B, Luo C, et al. High co-loading capacity and stimuli-responsive release based on cascade reaction of self-destructive polymer for improved chemo-photodynamic therapy. *ACS Nano* 2019;**13**:7010–23.
  84. Zhuang WR, Wang Y, Cui PF, Xing L, Lee J, Kim D, et al. Applications of  $\pi$ - $\pi$  stacking interactions in the design of drug-delivery systems. *J Control Release* 2019;**294**:311–26.
  85. Butterfield SM, Patel PR, Waters ML. Contribution of aromatic interactions to  $\alpha$ -helix stability. *J Am Chem Soc* 2002;**124**:9751–5.
  86. Koishi T, Yasuoka K, Ebisuzaki T, Yoo S, Zeng XC. Large-scale molecular-dynamics simulation of nanoscale hydrophobic interaction and nanobubble formation. *J Chem Phys* 2005;**123**:204707.
  87. Sun B, Luo C, Zhang X, Guo M, Sun M, Yu H, et al. Probing the impact of sulfur/selenium/carbon linkages on prodrug nano-assemblies for cancer therapy. *Nat Commun* 2019;**10**:1–10.
  88. Yan LT, Xie XM. Computational modeling and simulation of nanoparticle self-assembly in polymeric systems: structures, properties and external field effects. *Prog Polym Sci* 2013;**38**:369–405.
  89. Shamay Y, Shah J, İşık M, Mizrahi A, Leibold J, Tschaharganeh DF, et al. Quantitative self-assembly prediction yields targeted nanomedicines. *Nat Mater* 2018;**17**:361–8.
  90. Cho YW, Kim SY, Kwon IC, Kim IS. Complex adaptive therapeutic strategy (CATS) for cancer. *J Control Release* 2014;**175**:43–7.
  91. Chen Q, Liu G, Liu S, Su H, Wang Y, Li J, et al. Remodeling the tumor microenvironment with emerging nanotherapeutics. *Trends Pharmacol Sci* 2018;**39**:59–74.
  92. Komarova NL, Wodarz D. Drug resistance in cancer: principles of emergence and prevention. *Proc Natl Acad Sci U S A* 2005;**102**:9714–9.
  93. Mokhtari RB, Homayouni TS, Baluch N, Morgatskaya E, Kumar S, Das B, et al. Combination therapy in combating cancer. *Oncotarget* 2017;**8**:38022.
  94. Lane D. Designer combination therapy for cancer. *Nat Biotechnol* 2006;**24**:163–4.
  95. Wang K, Ye H, Zhang X, Wang X, Yang B, Luo C, et al. An exosome-like programmable-bioactivating paclitaxel prodrug nano-platform for enhanced breast cancer metastasis inhibition. *Biomaterials* 2020;**257**:120224.
  96. Wang Z, Song L, Liu Q, Tian R, Shang Y, Liu F, et al. A tubular DNA nanodevice as a siRNA/chemo-drug co-delivery vehicle for combined cancer therapy. *Angew Chem Int Ed* 2021;**60**:2594–8.
  97. Xu X, Ho W, Zhang X, Bertrand N, Farokhzad O. Cancer nanomedicine: from targeted delivery to combination therapy. *Trends Mol Med* 2015;**21**:223–32.
  98. Hu CMJ, Zhang L. Nanoparticle-based combination therapy toward overcoming drug resistance in cancer. *Biochem Pharmacol* 2012;**83**:1104–11.
  99. Tang W, Fan W, Lau J, Deng L, Shen Z, Chen X. Emerging blood–brain-barrier-crossing nanotechnology for brain cancer theranostics. *Chem Soc Rev* 2019;**48**:2967–3014.
  100. Li X, Kim J, Yoon J, Chen X. Cancer-associated, stimuli-driven, turn on theranostics for multimodality imaging and therapy. *Adv Mater* 2017;**29**:1606857.
  101. Gong F, Yang N, Wang X, Zhao Q, Chen Q, Liu Z, et al. Tumor microenvironment-responsive intelligent nanoplatforams for cancer theranostics. *Nano Today* 2020;**32**:100851.
  102. Cole AJ, Yang VC, David AE. Cancer theranostics: the rise of targeted magnetic nanoparticles. *Trends Biotechnol* 2011;**29**:323–32.
  103. Yamashita K, McDaid J, Öllinger R, Tsui TY, Berberat PO, Usheva A, et al. Biliverdin, a natural product of heme catabolism, induces tolerance to cardiac allografts. *FASEB J* 2004;**18**:765–7.
  104. Wegiel B, Gallo D, Cszmadia E, Roger T, Kaczmarek E, Harris C, et al. Biliverdin inhibits Toll-like receptor-4 (TLR4) expression through nitric oxide-dependent nuclear translocation of biliverdin reductase. *Proc Natl Acad Sci U S A* 2011;**108**:18849–54.
  105. Twelves C, Jove M, Gombos A, Awada A. Cytotoxic chemotherapy: still the mainstay of clinical practice for all subtypes metastatic breast cancer. *Crit Rev Oncol Hematol* 2016;**100**:74–87.
  106. Bocci G, Kerbel RS. Pharmacokinetics of metronomic chemotherapy: a neglected but crucial aspect. *Nat Rev Clin Oncol* 2016;**13**:659.
  107. Heym B, Honoré N, Schurra C, Cole S, Truffot-Pernot C, Grosset J, et al. Implications of multidrug resistance for the future of short-course chemotherapy of tuberculosis: a molecular study. *Lancet* 1994;**344**:293–8.
  108. Persidis A. Cancer multidrug resistance. *Nat Biotechnol* 1999;**17**:94–5.
  109. Schirmacher V. From chemotherapy to biological therapy: a review of novel concepts to reduce the side effects of systemic cancer treatment. *Int J Oncol* 2019;**54**:407–19.
  110. Wu H, Jin H, Wang C, Zhang Z, Ruan H, Sun L, et al. Synergistic cisplatin/doxorubicin combination chemotherapy for multidrug-resistant cancer via polymeric nanogels targeting delivery. *ACS Appl Mater Interfaces* 2017;**9**:9426–36.
  111. Garcia G, Odaimi M. Systemic combination chemotherapy in elderly pancreatic cancer: a review. *J Gastrointest Cancer* 2017;**48**:121–8.
  112. Liu Z, Zheng Q, Chen W, Wu M, Pan G, Yang K, et al. Chemosensitizing effect of Paris Saponin I on camptothecin and 10-hydroxycamptothecin in lung cancer cells via p38 MAPK, ERK, and Akt signaling pathways. *Eur J Med Chem* 2017;**125**:760–9.
  113. Bodley A, Liu LF, Israel M, Seshadri R, Koseki Y, Giuliani FC, et al. DNA topoisomerase II-mediated interaction of doxorubicin and daunorubicin congeners with DNA. *Cancer Res* 1989;**49**:5969–78.
  114. Pao W, Miller V, Zakowski M, Doherty J, Politi K, Sarkaria I, et al. EGF receptor gene mutations are common in lung cancers from “never smokers” and are associated with sensitivity of tumors to gefitinib and erlotinib. *Proc Natl Acad Sci U S A* 2004;**101**:13306–11.
  115. Zhu Z, Jia J, Lu R, Lu Y, Fu Z, Zhao L, et al. Expression of PTEN, p27, p21 and AKT mRNA and protein in human BEL-7402 hepatocarcinoma cells in transplanted tumors of nude mice treated with the tripeptide tyroservatide (YSV). *Int J Cancer* 2006;**118**:1539–44.
  116. Karagiannis GS, Condeelis JS, Oktay MH. Chemotherapy-induced metastasis: mechanisms and translational opportunities. *Clin Exp Metastasis* 2018;**35**:269–84.
  117. D’Alterio C, Scala S, Sozzi G, Roz L, Bertolini G. In Paradoxical effects of chemotherapy on tumor relapse and metastasis promotion. *Semin Cancer Biol* 2020;**60**:351–61.
  118. Lv W, Chen N, Lin Y, Ma H, Ruan Y, Li Z, et al. Macrophage migration inhibitory factor promotes breast cancer metastasis via activation of HMGB1/TLR4/NF kappa B axis. *Cancer Lett* 2016;**375**:245–55.
  119. Ran S. The role of TLR4 in chemotherapy-driven metastasis. *Cancer Res* 2015;**75**:2405–10.
  120. Zhang T, Yang S, Du J. Protective effects of berberine on isoproterenol-induced acute myocardial ischemia in rats through regulating HMGB1–TLR4 axis. *Evid Based Complement Alternat Med* 2014;**2014**:849783.
  121. Dean-Colomb W, Esteva FJ. Her2-positive breast cancer: herceptin and beyond. *Eur J Cancer* 2008;**44**:2806–12.
  122. Pommier Y, Redon C, Rao VA, Seiler JA, Sordet O, Takemura H, et al. Repair of and checkpoint response to topoisomerase I-mediated DNA damage. *Mutat Res* 2003;**532**:173–203.
  123. Hsiang Y-H, Lihou MG, Liu LF. Arrest of replication forks by drug-stabilized topoisomerase I–DNA cleavable complexes as a mechanism of cell killing by camptothecin. *Cancer Res* 1989;**49**:5077–82.
  124. Ling YH, El-Naggar AK, Priebe W, Perez-Soler R. Cell cycle-dependent cytotoxicity, G2/M phase arrest, and disruption of p34cdc2/cyclin B1 activity induced by doxorubicin in synchronized P388 cells. *Mol Pharmacol* 1996;**49**:832–41.

125. Xie Z, Fan T, An J, Choi W, Duo Y, Ge Y, et al. Emerging combination strategies with phototherapy in cancer nanomedicine. *Chem Soc Rev* 2020;**49**:8065–87.
126. Celli JP, Spring BQ, Rizvi I, Evans CL, Samkoe KS, Verma S, et al. Imaging and photodynamic therapy: mechanisms, monitoring, and optimization. *Chem Rev* 2010;**110**:2795–838.
127. Pérez-Hernández M, Del Pino P, Mitchell SG, Moros M, Stepien G, Pelaz B, et al. Dissecting the molecular mechanism of apoptosis during photothermal therapy using gold nanoprisms. *ACS Nano* 2015;**9**:52–61.
128. Verissimo TV, Santos NT, Silva JR, Azevedo RB, Gomes AJ, Lunardi CN. *In vitro* cytotoxicity and phototoxicity of surface-modified gold nanoparticles associated with neutral red as a potential drug delivery system in phototherapy. *Mater Sci Eng C* 2016;**65**:199–204.
129. Hönigsman H. Phototherapy for psoriasis. *Clin Exp Dermatol* 2001;**26**:343–50.
130. Rao L, Bu LL, Xu JH, Cai B, Yu GT, Yu X, et al. Red blood cell membrane as a biomimetic nanocoating for prolonged circulation time and reduced accelerated blood clearance. *Small* 2015;**11**:6225–36.
131. Sun B, Chen Y, Yu H, Wang C, Zhang X, Zhao H, et al. Photodynamic PEG-coated ROS-sensitive prodrug nanoassemblies for core-shell synergistic chemo-photodynamic therapy. *Acta Biomater* 2019;**92**:219–28.
132. Luo C, Sun B, Wang C, Zhang X, Chen Y, Chen Q, et al. Self-facilitated ROS-responsive nanoassembly of heterotypic dimer for synergistic chemo-photodynamic therapy. *J Control Release* 2019;**302**:79–89.
133. Zhao D, Tao W, Li S, Li L, Sun Y, Li G, et al. Light-triggered dual-modality drug release of self-assembled prodrug-nanoparticles for synergistic photodynamic and hypoxia-activated therapy. *Nanoscale Horiz* 2020;**5**:886–94.
134. Wang T, Hu J, Luo H, Li H, Zhou J, Zhou L, et al. Photosensitizer and autophagy promoter coloaded ROS-responsive dendrimer-assembled carrier for synergistic enhancement of tumor growth suppression. *Small* 2018;**14**:1802337.
135. Robertson CA, Evans DH, Abrahamse H. Photodynamic therapy (PDT): a short review on cellular mechanisms and cancer research applications for PDT. *J Photochem Photobiol, B* 2009;**96**:1–8.
136. Li X, Kwon N, Guo T, Liu Z, Yoon J. Innovative strategies for hypoxic-tumor photodynamic therapy. *Angew Chem Int Ed* 2018;**57**:11522–31.
137. Liu Y, Jiang Y, Zhang M, Tang Z, He M, Bu W. Modulating hypoxia via nanomaterials chemistry for efficient treatment of solid tumors. *Acc Chem Res* 2018;**51**:2502–11.
138. Mellman I, Coukos G, Dranoff G. Cancer immunotherapy comes of age. *Nature* 2011;**480**:480–9.
139. Liu X, Wang D, Zhang P, Li Y. Recent advances in nanosized drug delivery systems for overcoming the barriers to anti-PD immunotherapy of cancer. *Nano Today* 2019;**29**:100801.
140. Song W, Musetti SN, Huang L. Nanomaterials for cancer immunotherapy. *Biomaterials* 2017;**148**:16–30.
141. Galluzzi L, Vacchelli E, Bravo-San Pedro JM, Buqué A, Senovilla L, Baracco EE, et al. Classification of current anticancer immunotherapies. *Oncotarget* 2014;**5**:12472.
142. Wang T, Wang D, Yu H, Feng B, Zhou F, Zhang H, et al. A cancer vaccine-mediated postoperative immunotherapy for recurrent and metastatic tumors. *Nat Commun* 2018;**9**:1–12.
143. Jeanbart L, Swartz MA. Engineering opportunities in cancer immunotherapy. *Proc Natl Acad Sci U S A* 2015;**112**:14467–72.
144. Fallon PG, Alcamí A. Pathogen-derived immunomodulatory molecules: future immunotherapeutics? *Trends Immunol* 2006;**27**:470–6.
145. Cheng B, Yuan WE, Su J, Liu Y, Chen J. Recent advances in small molecule based cancer immunotherapy. *Eur J Med Chem* 2018;**157**:582–98.
146. Massarelli E, William W, Johnson F, Kies M, Ferrarotto R, Guo M, et al. Combining immune checkpoint blockade and tumor-specific vaccine for patients with incurable human papillomavirus 16-related cancer: a phase 2 clinical trial. *JAMA Oncol* 2019;**5**:67–73.
147. Yang J, Hu L. Immunomodulators targeting the PD-1/PD-L1 protein-protein interaction: from antibodies to small molecules. *Med Res Rev* 2019;**39**:265–301.
148. Zak KM, Grudnik P, Magiera K, Dömling A, Dubin G, Holak TA. Structural biology of the immune checkpoint receptor PD-1 and its ligands PD-L1/PD-L2. *Structure* 2017;**25**:1163–74.
149. Valsecchi ME. Combined nivolumab and ipilimumab or monotherapy in untreated melanoma. *N Engl J Med* 2015;**373**:1270–70.
150. Phuengkham H, Ren L, Shin IW, Lim YT. Nanoengineered immune niches for reprogramming the immunosuppressive tumor microenvironment and enhancing cancer immunotherapy. *Adv Mater* 2019;**31**:1803322.
151. Zhao X, Subramanian S. Intrinsic resistance of solid tumors to immune checkpoint blockade therapy. *Cancer Res* 2017;**77**:817–22.
152. Galluzzi L, Humeau J, Buqué A, Zitvogel L, Kroemer G. Immunostimulation with chemotherapy in the era of immune checkpoint inhibitors. *Nat Rev Clin Oncol* 2020;**17**:725–41.
153. Heinhuis K, Ros W, Kok M, Steeghs N, Beijnen J, Schellens J. Enhancing antitumor response by combining immune checkpoint inhibitors with chemotherapy in solid tumors. *Ann Oncol* 2019;**30**:219–35.
154. Kuai R, Yuan W, Son S, Nam J, Xu Y, Fan Y, et al. Elimination of established tumors with nanodisc-based combination chemioimmunotherapy. *Sci adv* 2018;**4**:eaao1736.
155. Javeed A, Ashraf M, Riaz A, Ghafoor A, Afzal S, Mukhtar MM. Paclitaxel and immune system. *Eur J Pharm Sci* 2009;**38**:283–90.
156. Zhang L, Dermawan K, Jin M, Liu R, Zheng H, Xu L, et al. Differential impairment of regulatory T cells rather than effector T cells by paclitaxel-based chemotherapy. *Clin Immunol* 2008;**129**:219–29.
157. Turubanova VD, Balalaeva IV, Mishchenko TA, Catanzaro E, Alzeibak R, Peskova NN, et al. Immunogenic cell death induced by a new photodynamic therapy based on photosens and photodithazine. *J Immunother Cancer* 2019;**7**:1–13.
158. Garg AD, Agostinis P. ER stress, autophagy and immunogenic cell death in photodynamic therapy-induced anti-cancer immune responses. *Photochem Photobiol Sci* 2014;**13**:474–87.
159. Min Y, Roche KC, Tian S, Eblan MJ, McKinnon KP, Caster JM, et al. Antigen-capturing nanoparticles improve the abscopal effect and cancer immunotherapy. *Nat Nanotechnol* 2017;**12**:877.
160. Yu S, Wang C, Yu J, Wang J, Lu Y, Zhang Y, et al. Injectable bio-responsive gel depot for enhanced immune checkpoint blockade. *Adv Mater* 2018;**30**:1801527.
161. Hu L, Cao Z, Ma L, Liu Z, Liao G, Wang J, et al. The potentiated checkpoint blockade immunotherapy by ROS-responsive nanocarrier-mediated cascade chemo-photodynamic therapy. *Biomaterials* 2019;**223**:119469.
162. Liu M, Acres B, Balloul J-M, Bizouarne N, Paul S, Slos P, et al. Gene-based vaccines and immunotherapeutics. *Proc Natl Acad Sci U S A* 2004;**101**:14567–71.
163. Pastor F, Berraondo P, Etxeberria I, Frederick J, Sahin U, Gilboa E, et al. An RNA toolbox for cancer immunotherapy. *Nat Rev Drug Discov* 2018;**17**:751–67.
164. Lin Y-X, Wang Y, Blake S, Yu M, Mei L, Wang H, et al. RNA nanotechnology-mediated cancer immunotherapy. *Theranostics* 2020;**10**:281.
165. Sayour EJ, Grippin A, De Leon G, Stover B, Rahman M, Karachi A, et al. Personalized tumor RNA loaded lipid-nanoparticles prime the systemic and intratumoral milieu for response to cancer immunotherapy. *Nano Lett* 2018;**18**:6195–206.
166. Glas M, Coch C, Trageser D, Daßler J, Simon M, Koch P, et al. Targeting the cytosolic innate immune receptors RIG-I and MDA5 effectively counteracts cancer cell heterogeneity in glioblastoma. *Stem Cells* 2013;**31**:1064–74.
167. Li Y, Yue T, Yang K, Zhang X. Molecular modeling of the relationship between nanoparticle shape anisotropy and endocytosis kinetics. *Biomaterials* 2012;**33**:4965–73.